Offshore wind power potential and capacity density assessment in Utsira Nord

Katherina Sørensen Tyssekvam

Thesis for Master of Science Degree at the
University of Bergen, Norway

2024

Year: 2024
Title: Offshore wind power potential and capacity density assessment in Utsira Nord
Author: Katherina Sørensen Tyssekvam

Acknowledgements

I would like to thank my internal supervisor, Birgitte Rugaard Furevik, and my external supervisor, Lene Eliassen, for their support throughout my master's thesis. I also want to thank friends and family for all the encouragement and love. Finally, heartfelt thanks to my classmates for these two great years together.

Abstract

Optimizing offshore wind farm design with regard to minimal wake loss is important to ensure the success of offshore wind projects, as well as effective utilization of ocean resources. The thesis study the offshore wind power potential in Utsira Nord, by investigating how capacity expansion and turbine distance affect wake loss. The analysis is carried out using the modular wind farm and wake modelling Python package FOXES for different wind farm layouts. The results reveal that the common practice of using a constant turbulence intensity of 5% overestimates the power production compared to using calculated turbulence intensity from given wind data, with increasing deviations for increasing installed capacity. Furthermore, comparing three scenarios of different installed capacities proposed by the government and NVE suggests that adding an additional project area is a more energy-efficient method of capacity expansion than increasing the number of turbines within existing project areas, due to the dominant internal wake loss. A capacity density analysis for the three scenarios reveal decreasing internal and increasing external wake loss for growing turbine distance, as the wind farm size expand and cause less distance between the areas. In contrast, using full utilization of the designated areas result in both internal and external wake reduction as the turbine distance grow. The overall wake loss decreases in both cases, with significant improvement in the lower range of 2D-7D, while the effects gradually becomes less significant in the upper range for 8D-15D. A constant turbine distance of 7D is shown to provide a good balance between high power production and relatively low wake loss. An alternative farm layout that consider the dominating wind direction cause further wake loss reductions.

Contents

Chapter 1

Introduction

With pressing environmental issues and rising energy demands, renewable energy has become one of the most relevant endeavours for research in the energy industry. Apart from solar power, wind energy is the fastest-growing renewable energy source in terms of capacity additions from 2017 to 2022 stated by International Energy Agency (2024). While onshore wind power production is more established technology, offshore wind has seen substantial growth the past years and is expected to continue expanding in accelerated pace (Global Wind Energy Council (2024)). Offshore wind farms benefit from stronger and more consistent wind resources available at sea, offering more consistent production of greater power. However, offshore wind projects are significantly more expensive to install and maintain due to the marine environment.

Optimization of wind farm design is decisive for the success of offshore wind projects. A normal approach is to optimize revenue of the invested capital, by considering both investment and operational costs as well as the power production. Important parameters for optimization of offshore wind farm layouts include water depths and bottom sediment characteristics, distance to shore, anchoring and cable lengths, wind conditions and wake effects (Nielsen (2024), page 340). For a comprehensive evaluation of optimal wind farm design, considerations beyond technical optimization are also necessary, such as protection of the environment and interaction with other marine activities in the area. Given that the ocean serve as valuable resources for other industries such as fishing and shipping, it is important to ensure effective utilization of ocean resources. In this context, a pivotal aspect of the optimization process is maximizing power production and minimize power loss for a given wind farm area, to ensure both financial feasibility of offshore wind projects as well as optimal utilization of the area. Optimal turbine distance is imperative for achieving this, which is the focus of this study.

The density of turbines and their placement within a wind farm has a major influence on the wind farm performance, as their aerodynamic interactions are the primary source of energy loss (Nouri et al. (2022)). Wind turbines extract energy from the incoming wind and create a downstream airflow of reduced wind speed and increased turbulence that is called wake. Wind turbines that are placed in the wake of upstream turbines have less available energy from the incoming wind, leading to reduced efficiency. To optimize the wind farm efficiency, the design of a wind farm need to minimize the overall exposure to wake from upstream turbines. The capacity density, determined by the distance between each turbine, is a decisive parameter in this context as the intensity of the wake dissipate with distance from the rotor. Distance between neighbouring wind farm clusters is also of increasing significance as the wake of an offshore wind farm extend tens of kilometers downstream and the ongoing capacity expansion of offshore wind energy entails an increase in wind farm clusters. Hence, the design of future wind farms must consider both interactions of turbines within the wind farms as well as influence from neighbouring wind farm clusters to achieve optimal power output.

Utsira Nord is one of two areas that was opened for applications for renewable energy production at sea by the Norwegian government in 2021 (The Royal Ministry of Petroleum and Energy (2023)). In May 2022, the government presented an ambition of allocating 30 GW offshore wind production by 2040, which correspond to about 1500-2000 offshore wind turbines and is almost equivalent to the total power production in Norway today. The 1010 km^2 area of Utsira Nord is located along the Norwegian coast in the North Sea, about 22 km outside Rogaland. From the strategic impact assessment conducted by The Norwegian Water Resources and Energy Directorate (2012a), the wind conditions at Utsira Nord are good for wind power production compared to other areas along the Norwegian coast. This constitute a high net capacity factor of 47%, according to Norwegian Institute for Nature Research (2012), which is a measure of how much power is generated compared to what is theoretically possible (International Energy Agency (2021)). Further information about the area is listed in Table 1.1. Depths from 185 to 280 meters makes the area more suitable for floating wind turbines (The Norwegian Water Resources and Energy Directorate (2012a)). In June 2020 the ministry presented the opening decision for Utsira

Nord, which divide the area into three project areas with an installed power of 460-500 MW each (The Norwegian Government). In retrospect, NVE have suggested a capacity expansion of 250 MW for each project area (The Norwegian Government). There is a 5 km distance between the areas that enables through-going maritime traffic. The capacity density range for the development in the project area is 3.5-7.5 MW/km^2 (The Royal Ministry of Petroleum and Energy (2023)).

Vestavind F is an area expansion of Utsira Nord, Fig. 1.1, and is one of 20 areas that in April 2023 was suggested for offshore wind power assessment by NVE, in consultation with a directorate group (The Norwegian Water Resources and Energy Directorate (2018)). These regions are part of an ongoing expert analysis, including an assignment to divide Vestavind F in project areas beyond the existing ones in Utsira Nord. For a potential project area north of Utsira Nord, there is set requirements for a minimum installed capacity of 500 MW with a 5 km buffer zone from the existing project areas. For the remaining area of Vestavind F, either a western expansion of the existing three project areas or a new independent project area in the south is proposed. A minimal capacity density of 3.5 MW/km^2 is still applicable. Further details about Vestavind F are listed in Table 1.1.

Table 1.1: Utsira Nord and Vestavind F Parameters

Parameter	**Value**	**Unit**
Total area Utsira Nord	1010	km^2
Total area Vestavind F	1989	km^2
Distance to coastline	22	km
Depth	185-280	m
Average wind speed	10.2	m/s
Net capacity factor for 500 MW installation	48	%
Net capacity factor for 1500 MW installation	47	%

Sources:
The Norwegian Water Resources and Energy Directorate (2012b)
The Norwegian Water Resources and Energy Directorate (2023)

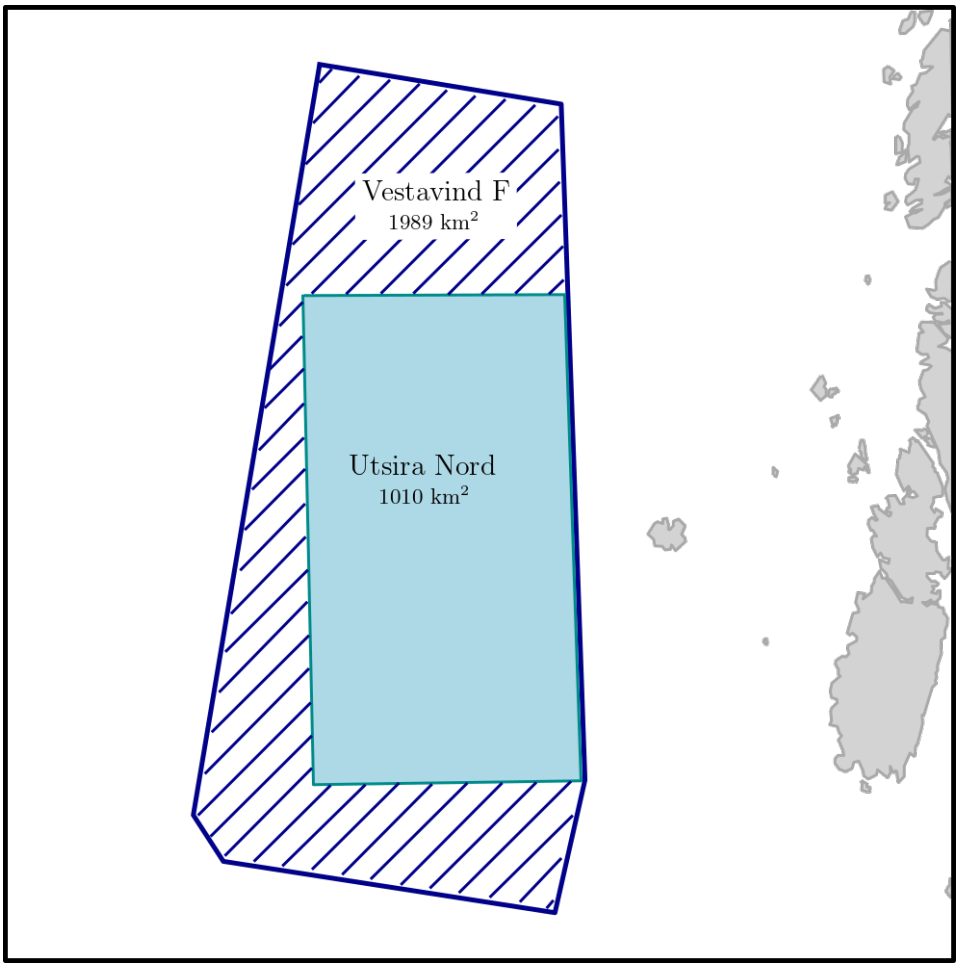

Figure 1.1: Vestavind F and Utsira Nord.
Inspired by: The Norwegian Water Resources and Energy Directorate (2023)

Part of the challenge in modelling offshore wind farms lies in obtaining accurate information about the wind conditions in offshore areas. A hindcast model like the 3-km Norwegian Reanalysis (NORA3), Haakenstad et al. (2021), can help address this challenge by providing valuable insight into the wind characteristics in areas with insufficient observations such as Utsira Nord. NORA3 is a high-resolution atmospheric dynamic downscaled data set that offer the first kilometer-scale climatological description of the North Sea, the Norwegian Sea and the Barents sea using nonhydrostatic model physics. NORA3 is created by the nonhydrostatic numerical weather prediction model HARMONIE–AROME, which downscale reanalysis data, ERA5, from ECMWF using a horizontal resolution of 3 km. The validation of NORA3 for wind power estimates conducted by Solbrekke et al. (2021) underscores the credibility of the data and suggests promising prospects for its future applications.

Turbulence intensity is an important input in engineering wake modelling, but is not provided by mesoscale modelling. In wind farm simulations of offshore scenarios, its common practice to use a constant turbulence intensity of 5%. An expression for turbulence intensity is derived by Larsén (2022) from mesoscale model output information on wind speed, height and turbulent kinetic energy. This enables the incorporation of seasonal variations in turbulence intensity into wind farm modeling.

To summarize, offshore wind energy is of significant interest due to its stronger and more consistent wind resources compared to onshore wind. The optimization of offshore wind farm design is crucial for economic viability, as these projects are more costly to install and maintain. Optimal wind farm design is a complex challenge, but focusing on maximizing power production for a given area while minimizing wake losses is essential for efficient utilization of marine resources. This is the main focus of the present study. Utsira Nord, recently opened for offshore wind development by the Norwegian government, serves as the case study area. Utilizing high-resolution wind data from the NORA3 dataset, this study investigates the offshore wind power potential at Utsira Nord.

1.1 Problem Statement and Objectives

The thesis study the offshore wind power potential in the Utsira Nord area, with an objective to investigate how capacity expansion and turbine distance affect wind farm wake effects. The aim is to determine the optimal distance between turbines within a wind farm at Utsira Nord with regard to maximum power production and minimal wake loss, while considering the specific characteristics of the area.

The analysis is carried out using a combination of NORA3 wind data and IEA 15-MW wind turbine data. The modular wind farm and wake modelling Python package FOXES is applied for two approaches considered in the thesis.

The first approach challenge the turbine density and placement with three scenarios of constant installed capacity. Thus for each of the three scenarios the area occupied by the wind farm varies with turbine distance while the number of turbines is constant. The first scenario is based on the 2020 announced proposition of 1380-1500 MW, while the second scenario investigate NVEs suggestion of a capacity expansion to 2250 MW for the same area. The third scenario take inspiration from the 2023 proposal from NVE that is based on the area Vestavind F, where the installed capacity is set to 3000 MW. This approach provide information about wake loss both within and between the government announced project areas for different capacity densities and turbine placements, and represent a feasible power potential for the area.

The second approach diverges from the announced capacities and rather utilize the entire available area of Utsira Nord both with and without project areas. Hence, the wind farm area is constant while the installed capacity vary with the number of turbines. This approach allow for an investigation of the effects on wind farm performance from capacity expansion and provide a comparison of the government defined division of the area with a uniform wind farm.

Chapter 2

Theory

This chapter outlines the basic principles of offshore wind energy production, focusing on wake effects and wake modelling. Special emphasis is placed on the theory behind the TurbOPark wake model, as this is employed in the simulations. Thereafter, the chosen simulation tool FOXES is presented with the relevant model choices and procedures. Finally, a brief overview of wind farm design parameters that affect wake effects is provided, focusing on capacity density, wind farm size and wake control strategies.

2.1 Wind Power Production

Understanding the principles of wind energy production is important to enable informed decisions in the modelling process of a wind farm. Wind turbines extract kinetic energy from the atmosphere, converting it into electrical energy (Jacobson & Archer (2012)). The power extracted from a wind turbine depend on the rotor diameter and the local wind characteristics

$$P = \frac{1}{2} \cdot C_P(U) \cdot \rho \cdot A \cdot U^3, \tag{2.1}$$

where ρ is the air density and A is the rotor area of the wind turbine. C_P is the power coefficient, which is the fraction of the theoretical maximum power that is actually generated to electrical power. The upstream wind speed U represent the energy resource for wind production, with stronger and more stable wind conditions being favourable for optimal power generation. The maximum possible power generation is defined by the Betz Limit of $C_{Pmax} \approx 0.59$, after Betz (1926).

The wind imposes loads on the turbine that must be considered to ensure efficient and safe operation. Each wind turbine has a range of wind speeds for power production, defined by a cut-in wind speed, a rated wind speed and a cut-out wind speed. The cut-in wind speed is the minimal wind speed for power production, while the rotor will shut down for wind that exceed

the cut-out wind speed to avoid structural damage. The rated wind speed is the average wind speed at which a turbine is designed to produce its nominal power output. This range can be illustrated by the turbines power curve, illustrated for the IEA 15-MW wind turbine in Fig. 2.1 with a cut-in wind speed of 3 m/s, a rated wind speed of 10.6 m/s and a cut-out wind speed of 25 m/s. When the incoming wind speed is between rated and cut-out wind speed, the angle of the turbine blades are adjusted to maintain nominal power output. This is called pitch control, which reduce the aerodynamic forces on the blades to protect the wind turbine from damage (Schubel & Crossley (2014)).

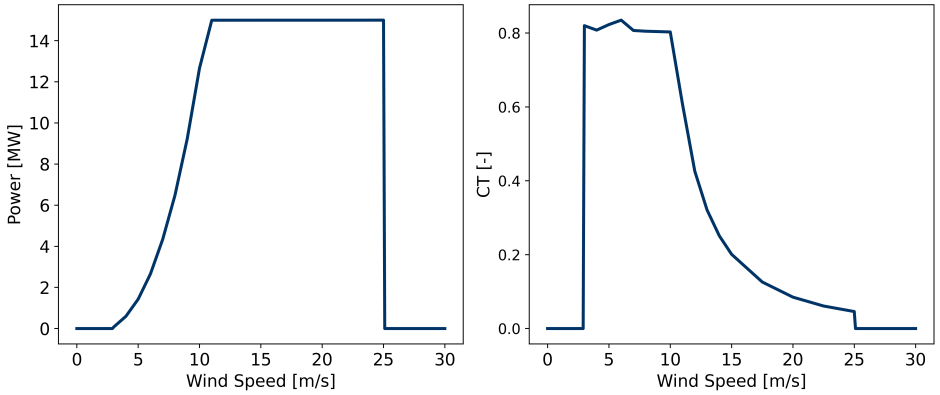

Figure 2.1: IEA 15-MW reference turbine power curve to the left and thrust curve to the right.
Source: Gaertner et al. (2020)

The incoming wind apply an axial force onto the wind turbine rotor. The thrust of a wind turbine refers to the counter force exerted by the rotor on the incoming wind, as it extract energy from it. The thrust coefficient C_T is a dimensionless parameter that represent the relation between the turbine thrust and the potential thrust available from kinetic energy in the incoming wind. Each turbine has a thrust curve that show the thrust coefficient as a function of wind speed (Fig. 2.1). Thrust is important for many engineering models as it describe the downstream flow of a turbine. Higher thrust indicate more energy captured by the turbine, leaving less energy in the downstream flow, which create more intense wake effects. In contrast, a low thrust coefficient indicate less energy captured and thereby less wake effects downstream.

2.2 Wake Theory

Wake effects are the primary source of power loss in wind power production, estimated as 10-20% for large offshore wind farms by Barthelmie et al. (2009). As the turbine extract energy from the wind, a wake characterised by reduced wind speed and increased turbulence is created downstream. Reduced wind speeds cause less energy available for the turbines impacted by the wake, while increased turbulence cause enhanced fatigue loads that reduce their lifespan and increase operation and maintenance costs. The wake area is often separated in two main categories, near field wake and far field wake. The near field wake is closer to the turbine rotor, assumed to extend two to four rotor diameters downstream by Porté-Agel et al. (2020). The near field differ from the far field with greater influence from the immediate aerodynamics of the turbine, which diminish with downstream distance as shear and turbulence cause mixing of the flow (Nielsen (2024), page 342). This entails decreasing velocity deficit with increasing distance from the rotor, and a conically wake shape downstream.

The level of atmospheric turbulence affect the wake recovery as increased turbulence intensity fosters enhanced mixing, which enable accelerated wake expansion and wind speed recovery (Gayle Nygaard et al. (2020)). The atmospheric turbulence levels is dependent on atmospheric stability. An unstable atmosphere can be characterised by increased turbulent mixing, while under stable conditions turbulent mixing is suppressed (Barthelmie & Jensen). Turbulence intensity is defined as the standard deviation of the wind speed σ_i in the mean wind direction divided by the mean wind speed $\bar{U}$ (Nybø et al.)

$$I_0 = \frac{\sigma_i}{\bar{U}}. \tag{2.2}$$

Wakes are not only a problem within wind farms, they also extend to the far field downstream. Wind farm wake is the collective effect of the turbine wakes, which is expected to extend much longer than the wake of single turbines (Porté-Agel et al. (2020)). The extension of wind farm wake is very dependent on the atmospheric stability and the turbulence levels. The small surface friction and weak temperature gradients of the ocean causes less turbulence production than over rough land surfaces, allowing the wake

to propagate over longer distances. Thereby, the generally more stable atmospheric conditions at sea (Nielsen (2024), page 340) cause wakes from offshore wind farms to extend further than from land-based wind farms, predicting wake lengths up to 100 km from analytical and numerical flow models (Platis et al. (2018)). Wind farm wake is measured to be 55 km long at Belwind wind farm, 45 km at Thornton Bank, 15 km at London Array, 14 km at Thanet and 10 km at Kentish Flat, all located in the southern North Sea (Hasager et al. (2015)).

There are many processes that affect the wake in a wind farm. The presence of a wind turbine also affect the wind in front of the rotor, called *induction effect*. The induction effect is found to reduce the incoming wind speed as the turbine rotor extract energy from the wind (Simley et al. (2016)). The front turbine row in a wind farm can experience significant reductions in wind speed for the middle turbines, while the turbines along the edges of the row experience increased wind speeds (Porté-Agel et al. (2020)). Another phenomenon is wake meandering, which is lateral motion in the trajectory of the wake (Larsen et al. (2007)). Wake meandering further complicates the prediction of wake effects, as it can cause downstream turbines to move partially or fully in and out of wake from upstream turbines. Thereby, accurate prediction and modelling of wake effects is a complex problem that require analysis in a large range of time and spatial scales. Detailed flow modelling can be very computationally demanding, but a number of simplified wake models have been developed over the years.

2.3 Engineering Wake models

Numerous engineering wake models have been developed to estimate wakes using algebraic equations, aiming to provide an accurate description that is computational inexpensive. The wake loss of an offshore wind farm is analysed using far field models, as the turbine distance normally exceeds five rotor distances (Nielsen (2024), page 342). First, the wake intensity from one wind turbine is calculated, followed by the superposition of wakes from several wind turbines. The wake model proposed by Jensen, Jensen (1983) Katic et al. (1987), also know as the Park wake model, is one of the oldest and most widely utilized models for simulating the velocity deficit in

wind farm layout optimization studies (Parada et al. (2017)). The model is derived by conservation of momentum downstream of a wind turbine and assumes a top-hat shape for the velocity deficit in the wake, characterised by a linearly expanding wake with a velocity deficit that only depends on the distance from the rotor. The Park model is shown to underestimate the wake loss from cluster wakes by more than 20% by Pedersen et al. (2022).

In 2014, Bastankhah & Porté-Agel (2014), developed an extension of the Jensen model that replace the top-hat profile with a Gaussian wake profile that is physically more appropriate and provide a better description of the instantaneous wake cross section. From Parada et al. (2017), the top-hat models generally overestimate the velocity deficit in the center of the wake and under-predict it towards the edges of the wake, while the Gaussian wake model is in acceptable agreement with LES simulations and wind tunnel measurements. The Bastankhah model is consistent and more accurate for power estimation compared to the Jensen wake model and other top-hat models. It does however not consider the effect of inflow conditions such as ambient turbulence intensity on the wake expansion parameter.

A wake model that does consider the incoming ambient turbulence intensity is the Turbulence Optimized Park model (TurbOPark). TurbOPark was developed with an objective to accurately capture the effect of both internal wind farm wakes and cluster wakes from neighbouring wind farms extending over long distances. The beta-version of TurbOPark, Gayle Nygaard et al. (2020), has a top-hat wake shape and use the same wind speed deficit as the Jensen model, but propose a locally linear wake expansion with an expansion rate determined by the local turbulence intensity in the wake and a model calibration constant A. The beta-version of TurbOPark is demonstrated to capture cluster wakes much better than the Park model from Gayle Nygaard et al. (2020). In comparison with the Jensen model and several other wake models, the beta TurbOPark captures the wind farm wake recovery observed in the LES more accurately and have a more accurate representation of the power production as a function of downstream direction Stieren & Stevens (2021). According to Al Halabi (2023) it better predicts the power production and variation compared to the Bastankhah and the Jensen wake model from comparison to real data at Horns Rev 1.

The new version of TurbOPark, Pedersen et al. (2022), differ from the beta-version with a Gaussian wind speed deficit model formulated by Bastankhah & Porté-Agel (2014)

$$\frac{\Delta U}{U_0} = \frac{U_0 - U_w}{U_0} = C(x) \cdot exp\left(-\frac{r^2}{2 \cdot \sigma_w^2(x)}\right), \tag{2.3}$$

where U_0 is the free stream wind speed at the position of the rotor generating the wake, U_w is the wind speed in the wake, r is the radial distance from the wake centre line and x is the downstream distance from the rotor. $C(x)$ is the peak deficit at the centre line of the wake

$$C(x) = 1 - \sqrt{1 - \frac{C_T(U_{in})}{8(\sigma_w(x)/D)^2}}, \tag{2.4}$$

where C_T is the thrust coefficient, U_{in} is the inflow wind speed, D is the rotor diameter and σ_w is the characteristic wake width

$$\frac{\sigma_w(x)}{D} = \varepsilon + \frac{A \cdot TI}{\beta}\left(\sqrt{\left(\alpha + \frac{\beta \cdot x}{D}\right)^2 + 1} - \sqrt{1 + a^2} - \ln\left[\frac{\sqrt{\left(\alpha + \frac{\beta \cdot x}{D}\right)^2 + 1} + 1}{\alpha(\sqrt{1 + \alpha^2} + 1)(\alpha + \frac{\beta \cdot x}{D})}\right]\right). \tag{2.5}$$

Here, $\alpha = c_1 \cdot I_0$ and $\beta = c_2 \cdot I_0 \sqrt{C_T \cdot U_{in}}$, while $D \cdot \varepsilon$ is the characteristic wake width at $x = 0$. TurbOPark use the following expression for ε, from Bastankhah & Porté-Agel (2014)

$$\varepsilon = 0.25\left(\frac{1 + \sqrt{1 - C_T(U_{in})}}{2\sqrt{1 - C_T(U_{in})}}\right)^{1/2}. \tag{2.6}$$

The wind speed deficit of TurbOPark is illustrated for 4, 10, 20 and 40 rotor distances downstream of an IEA 15-MW turbine rotor in Fig. 2.2, together with the top-hat Jensen model, the gaussian Bastankhah model and a Bastankhah model for yawed conditions Bastankhah & Porté-Agel (2016).

The TurbOPark wake model predict the greatest wind deficit with increasing distance from the rotor. The improved version of TurbOPark is shown to predict the correct size of the power deficit in contrast to the Park model, according to Pedersen et al. (2022).

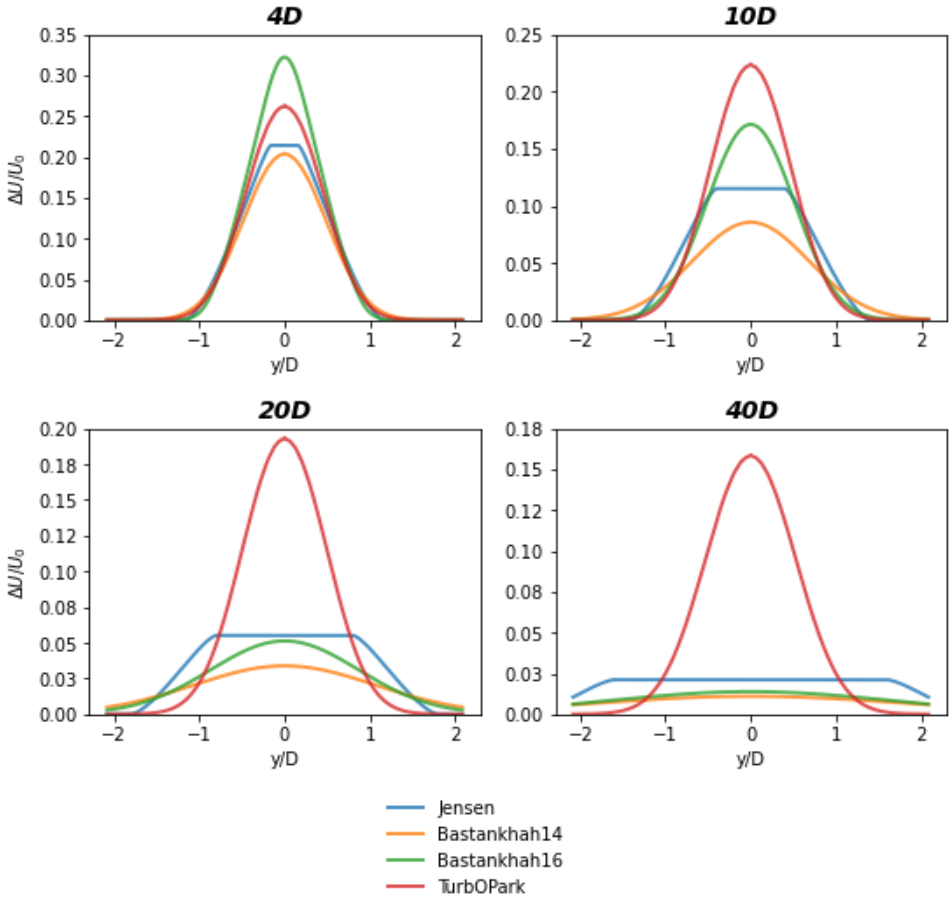

Figure 2.2: Comparison of wind speed deficit using the Jensen, Bastankhah 2014, Bastankhah 2016 and TurbOPark wake model for U=10.5 m/s, wd=270° and I_0=5%.

The non-linear wake expansion of TurbOPark is unique for this wake model

$$\frac{d\sigma_w}{dx} = A \cdot I(x). \tag{2.7}$$

The recommended value of the wake expansion calibration parameter A is found to be 0.04 for all offshore applications by Nygaard et al. (2022), based on validation of data from 19 offshore wind farms with an intention to model long distance wakes. The wake expansion is driven by a combination of the ambient, atmospheric turbulence and turbulence generated in the wake itself. The two sources of turbulence is added in quadrature

$$I(x) = \sqrt{I_0^2 + I_w^2(x)}. \tag{2.8}$$

The ambient atmospheric turbulence is characterized by the turbulence intensity I_0, defined in Eq. (2.2), while the turbulence generated in the wake itself I_w is modelled by an expression proposed by Frandsen (2007)

$$I_w(x) = \frac{1}{c_1 + c_2 \frac{x/D}{\sqrt{C_T(U_{in})}}}, \tag{2.9}$$

where $c_1 = 1.5$ and $c_2 = 0.8$ are empirically estimated constants. The wake generated turbulence depend on the turbine thrust coefficient C_T and decrease with increasing downstream distance x/D.

For a wind farm, the wake of the individual wind turbines must be added. Linear superposition, Lissaman (1979), is a common approach that assume linear expansion of the wakes, adding wake deltas as they come. Quadratic superposition, Katic et al. (1987), also called root square sum (RSS) model, is another common method that add the wake deltas quadratically and take the square root of the sum. Linear superposition can lead to negative wind speeds for large wind farms, while quadratic superposition avoid this problem.

2.4 FOXES

The Farm Optimization and eXtended yield Evaluation Software (FOXES) is a modular wind farm and wake modelling Python package developed by IWES, Schmidt et al. (2023). There are numerous applications available in FOXES, including wind farm simulation and optimization with complex model chains. The simulated Farm Power is based on Eq. (2.1) along with the provided power curve or Cp-curve for the chosen wind turbine and the specified wind speed, wind direction, and turbulence intensity from the given data. FOXES provides static data including thrust and power curves for multiple turbine models, listed in Table 2.1. The Farm Ambient Power is the power produced by the wind farm without accounting for any wake effects, utilizing the input wind speeds at rotor locations. Thereby, the wind farm wake loss is defined by the relation of the Farm Power P and the Farm Ambient Power AMB_P

$$Wake\ Loss = 1 - \frac{P}{AMB\_P} \cdot 100\%. \tag{2.10}$$

Turbine Type	**Source**
DTU 10MW reference turbine	Bak et al. (2013)
IEA 15 MW reference turbine	Gaertner et al. (2020)
IWES 7.5 MW reference turbine	Popko et al. (2018)
NREL 5 MW reference turbine	JM et al. (2009)

Table 2.1: Reference Wind Turbine Power and Thrust curves available in FOXES

The wind wake models available in the Foxes model book are listed in Table 2.2. The wake plots for a single turbine using the different wake models in Foxes are illustrated for long distances behind the rotor in Fig. 2.3 and closer to the rotor in Fig. 2.4. The simplified, linear expansion of the wake predicted by the Jensen model is apparent from both distances. The Bastankhah (2014) show the strongest wake effects in near proximity of the rotor, up to about 2D downstream. The TurbOPark model predict a stronger wake of less width for longer distances from about 8D downstream.

Wind Wake Model	Wake profile	Source
Jensen	Top Hat	Jensen (1983)
Bastankhah	Gaussian	Bastankhah & Porté-Agel (2014)
Bastankhah	Gaussian	Bastankhah & Porté-Agel (2016)
TurbOPark	Gaussian	Pedersen et al. (2022)

Table 2.2: Wind Wake Models available in FOXES

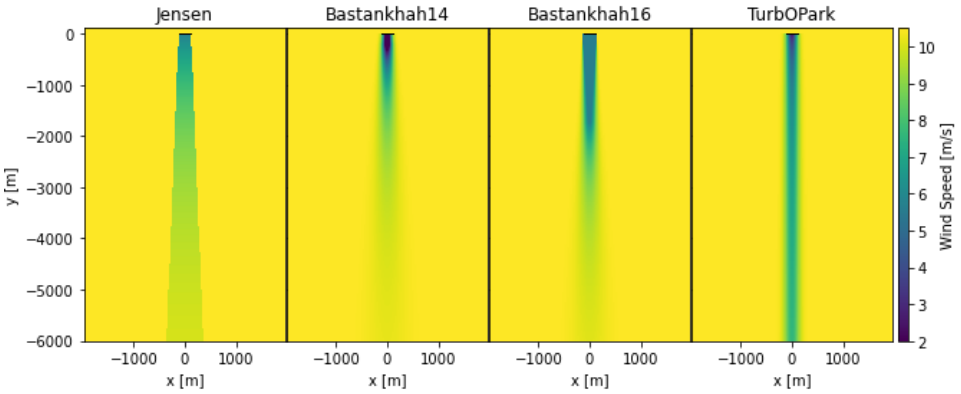

Figure 2.3: Comparison of long distance wake for a single IEA 15-MW turbine using Jensen, Bastankhah (2014), Bastankhah (2016) and TurbOPark wake model.

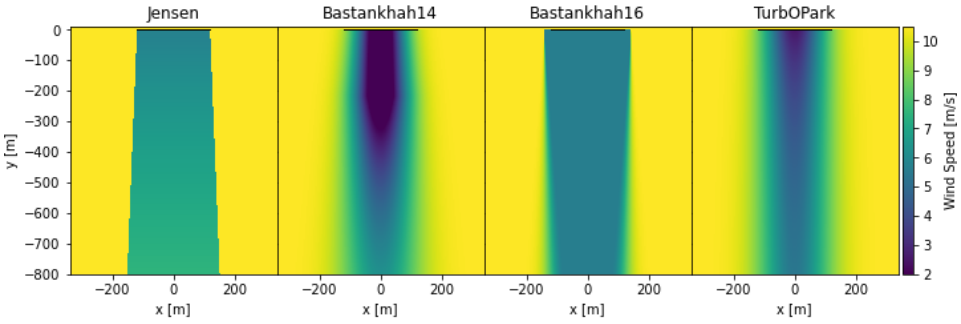

Figure 2.4: Comparison of wake with closer proximity to the rotor for a single IEA 15-MW turbine using Jensen, Bastankhah (2014), Bastankhah (2016) and TurbOPark wake model.

When choosing a wake model it is also required to choose a method of superposition for how the wakes are to be added. The available superpositions are listed in Table 2.3. Further information about the available superposition methods are described in Schmidt & Vollmer (2020).

Superposition model	**Source**
Linear	Lissaman (1979)
Quadratic	Katic et al. (1987)
Product	Lanzilao & Meyers (2022)
Max	Schmidt & Vollmer (2020)

Table 2.3: Wake superposition models available in FOXES

2.5 Wind Farm Design

Capacity density is an important wind farm design parameter with regard to wake effects and area utilization. Capacity density is defined as the installed capacity of the wind farm divided by the wind farm area, and is thereby determined by the number of turbines in a given region. Placing the turbines close together involves a high capacity density, entailing increased wake loss while allowing for more turbines in a given area. Increasing the distance between turbines reduce wake-induced power losses while reducing the number of turbines for a given area, and thus the power production. Typical turbine distances in existing wind farms are 6-10D (Stevens et al. (2016)). Horns Rev, the first large-scale offshore wind farm that was built in 2002 with 80 turbines and 160 MW, use a turbine distance of 7D. The second generation layout of Horns Rev 2 reduce the turbine distance to 5.4D (Giebel & Hasager (2016)), while the following wind farm of Horns Rev 3 use varying turbine distances between 6.1- 9.1D (Vattenfall).

Wind farm efficiency decrease with growing wind farm size for a given turbine distance. More turbines generate more wake effects, leading to greater power loss. Previous research suggest clusters of small to medium sized wind farms (25-342 km^2) rather than large wind farms ($28.9 \cdot 10^3$ - $114 \cdot 10^3$ km^2) for the wind conditions in the North Sea, due to significantly better wind farm efficiencies with sufficient distance between the clusters

(Volker et al. (2017)). The optimal wind farm design is dependent on the site-specific wind conditions. The wind strength is decisive for the optimal wind farm size, as stronger winds can cause sufficient efficiency also for larger wind farms, while the wind direction is important for other wind design parameters such as wind farm angle and turbine distances. Porté-Agel et al. (2013) found that a 10 degree change in wind direction can cause a 43% increase in power output. Hence, the orientation of the wind farm can have significant effects on the overall wake loss. The turbine placement should maximize the distance to downwind turbines for the dominant wind directions to allow optimal wake recovery for the most frequent wind conditions. Hence, lines of turbines in the direction of prevailing wind should be avoided.

In wind farms, different control strategies can be applied to manipulate the wake trajectory. Controlling the yaw angle, the angle between the direction of the wind and the direction of the turbine rotor, can be used to steer the wake away from downstream turbines. This can results in increased production and reduced fatigue loads for the affected turbine downstream, while the power production for the upstream turbine may be reduced (Nielsen (2024), page 349). Combining yaw control with wake steering and power control of the individual turbines can contribute to optimized wind farm power output, while simultaneously reducing turbine fatigue loads.

In summary, the theory chapter has provided an overview of important aspects of wind power production that offer insights into the wind farm modeling process. Knowledge about wake effects in offshore wind farms and fundamental principles and theories behind simplified wake models establish a basis for understanding the choices made in the modeling process.

Chapter 3

Methods and Data

This chapter describes the details of the modelling process. First, the wind resource data is presented. Subsequently, details of model- and variable choices for the wind farm simulation program FOXES are given. Finally, the chosen wind farm layouts for the two analytic approaches are displayed.

3.1 Wind Resource Data

The simulations are driven by wind resource data from the 3 km Norwegian reanalysis NORA3, Haakenstad et al. (2021). The data is obtained from the THREDDS Data Server (TDS), a web server that provides metadata and data access for scientific datasets. NORA3 encloses the majority of the northern part of the Atlantic Ocean with a 3x3 km horizontal grid and is created from down-scaling the state-of-the-art reanalysis data ERA5 that covers the Earth in an approximately 31×31 km horizontal grid. NORA3 provides valuable insights into the wind characteristics of the target offshore area, Utsira Nord.

The thesis use 3-hourly data from January 2000 to December 2022 with the coordinates 59.263°N, 4.131°E. Using 23 years of data is based on the approximate lifetime of a turbine, stated as 20-25 years by Skrzypiński et al. (2020). The simulations of this study use data for wind speed U, wind direction and turbulent kinetic energy TKE at 150 meters height as a time series input, except where noted otherwise.

Turbulence intensity is obtained from the derivation of its relationship with turbulence kinetic energy, performed by Larsén (2022). This method use mesoscale model output information on wind speed, height and TKE to obtain I_0

$$I_0 = \frac{1}{\bar{U}} \sqrt{\frac{2 \cdot TKE}{(1 + \alpha^{-1} + \beta^{-1})}}, \tag{3.1}$$

where σ_u is the standard deviation of the along wind component and $\bar{U}$ is the corresponding mean wind speed over the same time period. Alpha α and beta β are derived from using the Kaimal boundary-layer turbulence model, Kaimal & Finnigan (1994), with the resulting expressions for hub height at 150 m

$$\alpha = \frac{\sigma_u^2}{\sigma_v^2} = 1.78269 - \frac{0.556949}{U^{0.5}} + 0.000730406U, \tag{3.2}$$

$$\beta = \frac{\sigma_u^2}{\sigma_w^2} = 3.19169 - \frac{1.35477}{U^{0.5}} + 0.00196249U, \tag{3.3}$$

where U denotes the wind speed, while σ_v and σ_w is the standard deviation of the cross- and vertical wind component respectively.

These methods allow for the calculation of a turbulence intensity for each data point of the corresponding wind speed and wind direction, which together form a time series that can be used in the FOXES simulation tool.

3.2 Wind Farm Simulation Tools and Models

The modular structure of FOXES enables exploration of various parameters such as wind characteristics, turbine distances and capacity densities within various wind farm layouts, enabling a thorough analysis of their impact on overall energy production and efficiency. An overview of the selected simulation parameters are found in Table 3.1.

TurbOPark is chosen because of its ability to accurately capture wind farm wake recovery as well as its consideration of atmospheric turbulence intensity, making it the only wind wake model to partially account for the impact of atmospheric stability. The model is defined by two key inputs: the wake width parameter A and the chosen superposition method. As mentioned in

section 2.3 the wake width parameter is set to 0.04. Quadratic superposition is applied to follow the original setup of the model (Nygaard et al. (2022)). The offshore reference IEA 15-MW wind turbine, Gaertner et al. (2020), has a fixed-bottom monopile support structure and is chosen as the most suitable turbine choice for offshore conditions due to its larger rotor diameter and hub height. Consequently, floating wind turbines are not considered in this wind farm modelling. While Utsira Nord is designated for floating turbines, the main objective of this study is to investigate the effect of increasing installed capacity and turbine distance on wake loss and power potential. The fundamental trends observed in wake interactions and spacing are expected to be applicable, despite the use of a fixed-bottom turbine model. The power and thrust curve for the IEA 15-MW turbine are illustrated in Fig. 2.1.

Table 3.1: Selected parameters for the wind farm simulations.

Parameters	**Simulation parameter selection**
Wind Wake model	**TurbOPark** $A = 0.04$ Quadratic superposition
Wind Turbine	**IEA 15-MW** Horizontal axis Cut-in wind speed: 3 m/s Rated wind speed: 10.59 m/s Cut-out wind speed: 25 m/s Hub height: 150 m Rotor diameter: 240 m
Data	**NORA3 arome3km_3hr** Coordinates: 59.263°N, 4.131°E Time interval: 01.01.2000-31.12.2022 Height: 150 m

3.3 Wind Farm Layouts

This section present the wind farm layouts for the two approaches described in section 1.1. First, the three scenarios with constant installed capacities in Approach 1 are presented. The associated wind farm layouts are displayed, both with a constant turbine distance and with an alternative wind farm layout that consider the dominant wind direction for the turbine distance. Subsequently, the wind farm layouts for Approach 2 with full utilization of Utsira Nord with and without considering project areas are provided.

The wind farm layouts illustrate Vestavind F as a dotted line, Utsira Nord as a solid, black line and project area 1, 2, 3 and 4 in yellow, green, red and blue respectively.

3.3.1 Approach 1: Constant Installed Capacity

Scenario 1 (Initial Scenario) is based on the Norwegian government's opening decision for Utsira Nord. The ministry divides the area in three project areas of 460-500 MW each (The Royal Ministry of Petroleum and Energy (2023)) positioned with a 5 km distance between them in north-south direction. The wind farms in the Initial Scenario are hence constructed of 32 IEA 15-MW turbines (480 MW) for each project area, corresponding to a total installed capacity of 1440 MW. The northernmost project area is defined as Project area 1, the following as Project area 2 and the southernmost as Project area 3.

Scenario 2 (Capacity Expansion Scenario) is based on a capacity expansion to 750 MW for each project area, suggested by the Norwegian Directorate of Water Resources and Energy's (NVE) as an assignment from the Ministry of 9 February 2022 (The Royal Ministry of Petroleum and Energy (2023)). This is constructed as 50 IEA 15-MW turbines for each project area.

Scenario 3 (Area Expansion Scenario) represent NVEs suggestion of an area expansion for Utsira Nord to enable a better use of the area. The new identified area is Vestavind F of 1989 km^2, about twice the size of Utsira Nord of 1010 km^2 (The Norwegian Water Resources and Energy Directorate

(2023)). The boundaries of the fourth project area are based on requirements stated by NVE of a minimal distance of 5 km to the nearest project area, and follows the western boundary of Vestavind F in this study. Other requirements align with those for the original project areas with a minimum installed capacity of 500 MW. An installed capacity equivalent to the project areas of the Capacity Expansion Scenario is chosen for all project areas in the Area Expansion Scenario, allowing for an overall capacity increase as well as an impact assessment of adding an additional project area without changing the installed capacity per area.

Constant Turbine Distance

For a constant turbine distance, the wind farm layouts are constructed as 4x8 turbines for each of the three project areas in the Initial Scenario and 5x10 turbines for the three project areas in the Capacity Expansion Scenario and the four project areas in the Area Expansion Scenario. The turbine placements in the three scenarios are based on the angles of the south-west corners of the areas. Project area 2 is the most angled of the three in Utsira Nord and the self defined Project area 4 is the most angled overall.

The chosen horizontal rectangular layout, using twice as many turbines in each row horizontally as number of rows vertically, is beneficial in several ways. The design is better adapted the shape of the project areas compared to a quadratic or vertical rectangular layout, which allow for longer turbine distances while keeping within the borders of the areas. In addition, it has been demonstrated to have the smallest wake loss compared to alternative setups with the given data, listed in Table 3.2. The 9x4 layout have a vertical rectangular shape with four columns and nine rows of turbines, while opposite for the horizontal rectangular 4x9 layout. Using a horizontal rectangular layout is the best option for minimal wake loss out of the three presented layouts, both for a single wind farm and with two additional wind farms that are arranged in north-south direction.

First, a comparison of Scenario 1 (Initial Scenario), 2 (Capacity Expansion Scenario) and 3 (Area Expansion Scenario) is conducted using a seven rotor diameter (7D) distance between the turbines, as illustrated in Fig. 3.1. The turbine distance is based on a recommendation from The Norwegian Water

Layout	6x6	9x4	4x9
	Single Wind Farm		
Number of Turbines	36	36	36
Wake loss [%]	6.7	6.8	5.9
	Three Wind Farms		
Number of Turbines	108	108	108
Wake loss [%]	8.7	8.8	8.0

Table 3.2: Comparison of a quadratic, vertical rectangular and horizontal rectangular layout for Utsira Nord with a turbine distance of 7D.

Resources and Energy Directorate (2012b) in association with identification of relevant offshore wind areas along the Norwegian coast. Thereafter, the effects of different capacity densities are investigated by using various turbine distances. Turbine distances of 8D and more exceed the designated project areas for the Capacity Expansion and Area Expansion scenarios, illustrated in Fig. 3.2, corresponding with 10D or more for the Initial Scenario, illustrated in Fig. 3.3. From distances of 11D, Fig. 3.4, the wind farms in the Capacity Expansion and Area Expansion scenarios exceed the area of Utsira Nord and Vestavind F. The distance between the project areas decrease with increasing turbine distance, causing the outermost turbines from different project areas to get closer than the given turbine distance. For the Capacity and Area Expansion scenarios, this occurs at 13D, as shown in Fig. 3.5, eventually leading to turbine collisions at 15D, illustrated in Fig. 3.6. Therefore, farm results for turbine distances of 15D are excluded for these two scenarios.

The capacity assessment include turbine distances from 2D-15D for the Initial Scenario and 2D-14D for the Capacity Expansion and Area Expansion scenarios. From section 2.5, existing offshore wind farms use turbine distances that range from 5.4D to 10D. Hence, the lowest range of the turbine distances considered here are not deemed realistic. Similarly, the higher range of turbine distances will exceed the designated areas. Nevertheless, these distances are included in the analysis to study their effect on wake loss and to better understand the impact of increasing turbine distances.

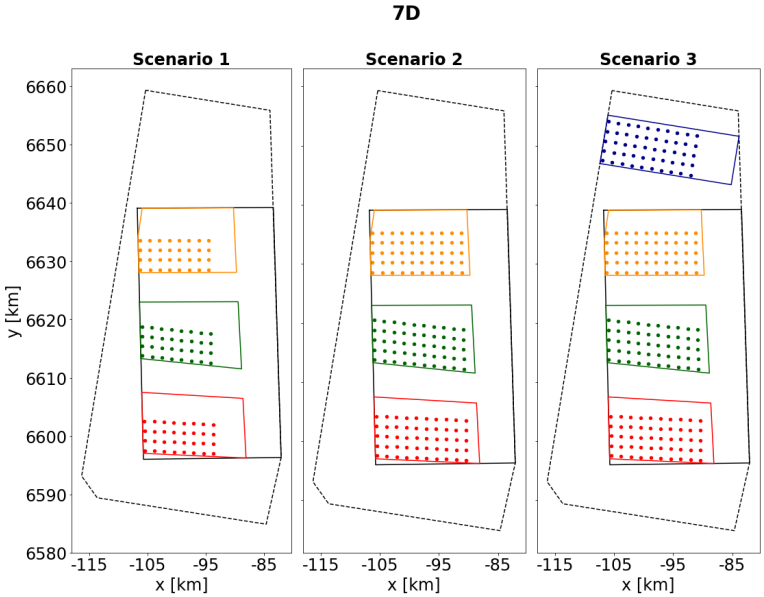

Figure 3.1: Scenario 1 (Initial Scenario), 2 (Capacity Expansion Scenario) and 3 (Area Expansion Scenario) with a turbine distance of 7D.

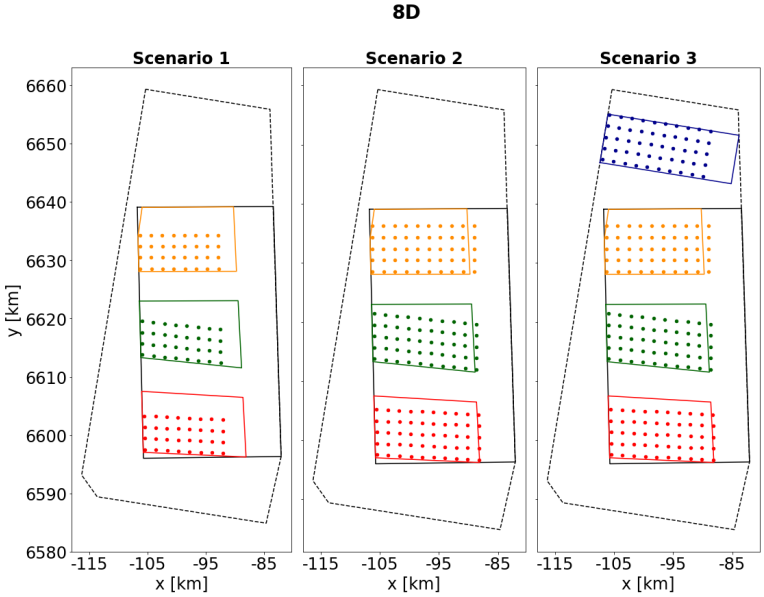

Figure 3.2: Scenario 1 (Initial Scenario), 2 (Capacity Expansion Scenario) and 3 (Area Expansion Scenario) with a turbine distance of 8D.

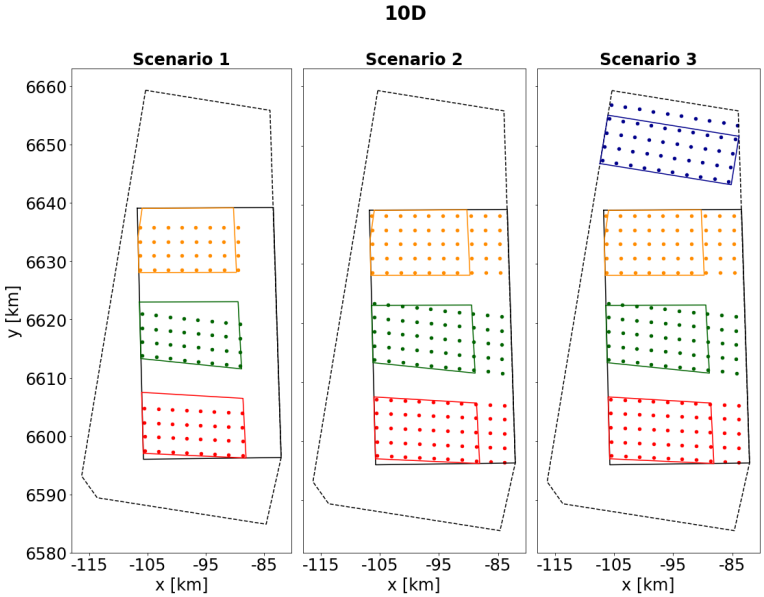

Figure 3.3: Scenario 1 (Initial Scenario), 2 (Capacity Expansion Scenario) and 3 (Area Expansion Scenario) with a turbine distance of 10D.

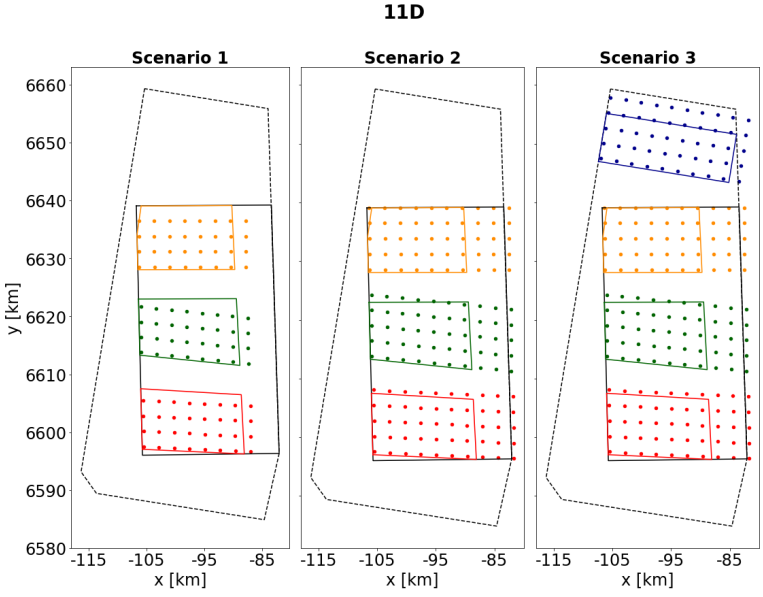

Figure 3.4: Scenario 1 (Initial Scenario), 2 (Capacity Expansion Scenario) and 3 (Area Expansion Scenario) with a turbine distance of 11D.

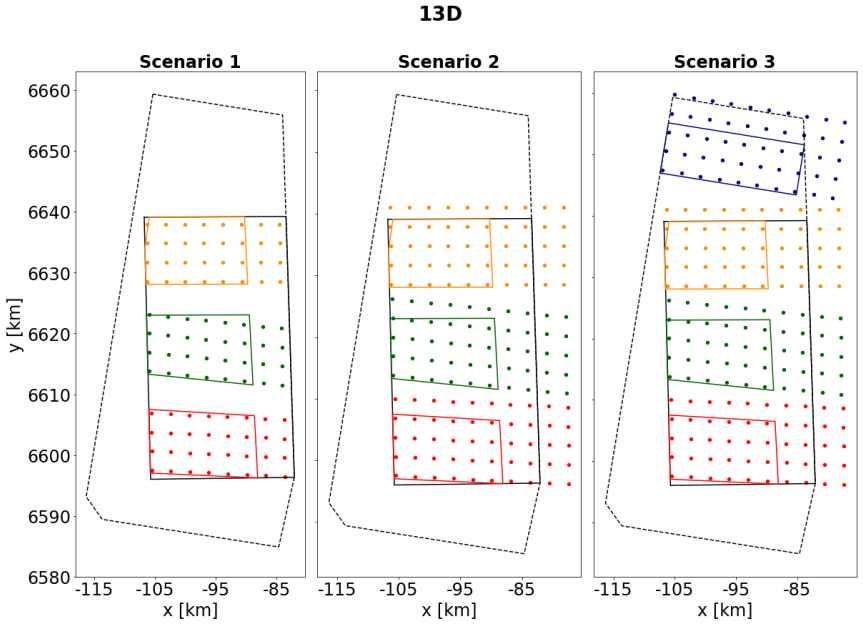

Figure 3.5: Scenario 1 (Initial Scenario), 2 (Capacity Expansion Scenario) and 3 (Area Expansion Scenario) with a turbine distance of 13D.

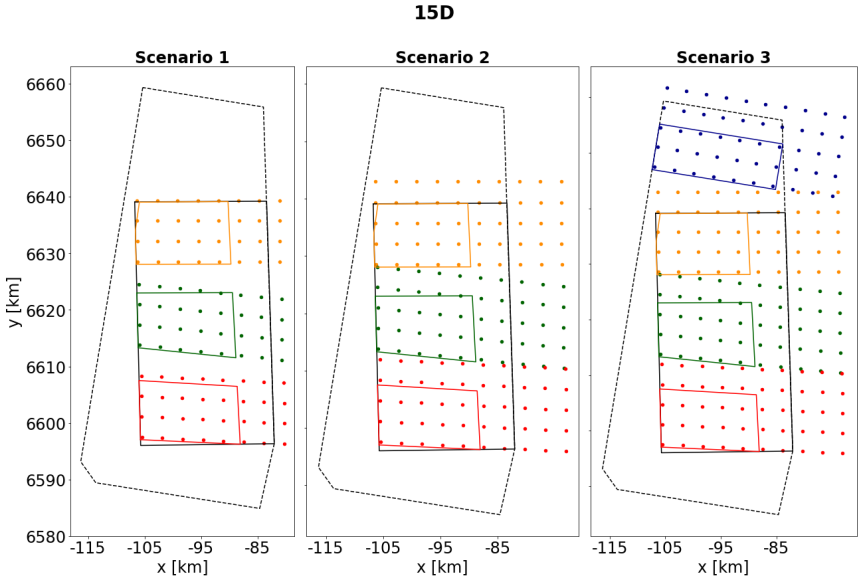

Figure 3.6: Scenario 1 (Initial Scenario), 2 (Capacity Expansion Scenario) and 3 (Area Expansion Scenario) with a turbine distance of 15D.

Alternative Wind Farm Layout

A constant distance between the turbines may not be optimal for an area with a dominant wind direction, such as Utsira Nord. Therefore, an alternative layout is suggested. From section 4.1 there is a dominant wind direction from north-northwest in Utsira Nord. Thereby, turbines will stand in the wake of upstream turbine rows more frequently than neighboring turbines in the same row. Hence, the turbines in each row are placed closer together, while the distance between the rows are increased. The turbine distances are inspired by a suggestion from The Norwegian Water Resources and Energy Directorate (2012b) of using five and nine rotor diameters for areas with dominating wind directions. The wind farms for each area are also separated in clusters with various distances between them, depending on the available area. The direction of the turbine rows is still determined by the boundaries of the project areas. The chosen layouts for Scenario 1 (Initial Scenario), 2 (Capacity Expansion Scenario) and 3 (Area Expansion Scenario) are illustrated in Fig. 3.7. The wind farm layouts are different for each project area, as the design of the area borders are different. This allow for a comparison of the various layout solutions by analogizing the resulting wake loss reduction for the individual project areas without the others presence.

For the Initial Scenario, the wind farms in each project area are separated in four clusters with a distance ranging from eight to almost ten kilometers in east-west direction and five to nearly seven kilometers in north-south direction. For the Capacity Expansion Scenario there is less empty space in north-south direction and the project areas are therefore mainly separated in two clusters with about seven kilometers distance in east-west direction. Project area 1 stands out with one turbine row along the northern border of the area, creating about four kilometers to the turbine row beneath. The additional project area for the Area Expansion Scenario is designed to be larger than the existing project areas of Utsira Nord for this thesis, as the area is not predefined by the government. This wind farm is thereby separated in four clusters of different sizes.

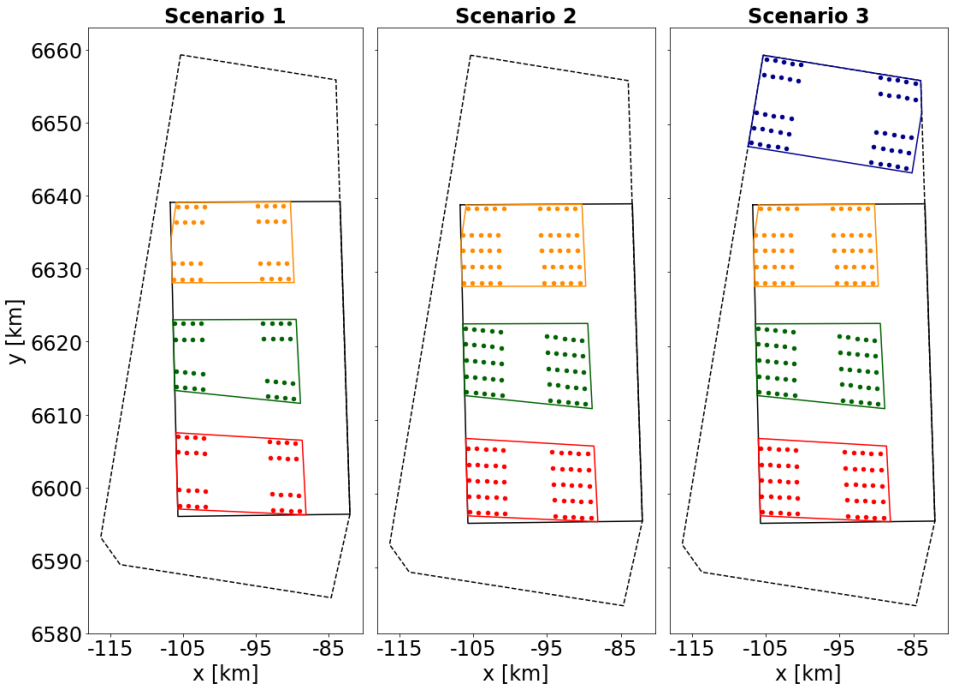

Figure 3.7: Alternative Wind Farm Layout for Scenario 1 (Initial Scenario), 2 (Capacity Expansion Scenario) and 3 (Area Expansion Scenario), using 5D within the turbine rows and 9D between them.

3.3.2 Approach 2: Full Area Utilization of Utsira Nord

This section present the chosen wind farm designs using as many rows of turbines as possible within Utsira Nord with and without considering project areas, using constant turbine distances. An overview of the wind farm layouts and the corresponding installed capacities for Utsira Nord with project areas are found in Table 4.5. The wind farms are illustrated in Fig. 3.8 and Fig. 3.9. The utilization rate will vary slightly with the turbine distance. The installed capacities range from 750 MW to 8475 MW, corresponding to a range from half of the installed capacity of the Initial Scenario to about 2-3 times the installed capacity of the Area Expansion Scenario. The wind farm layout does not follow the exact design of project area 1 but rather follow the outline of the upper left corner of Utsira Nord for simplicity. The total area of the rotor is not considered and the wind farms will slightly exceed the limits of the areas in some cases.

Table 3.3: Wind farm layout and installed capacity with full area utilization for Utsira Nord with project areas

	Wind Farm Layout			**Installed Capacity**
	Project area 1	Project area 2	Project area 3	[MW]
4D	11x17	10x18	11x18	8475
5D	9x14	8x14	9x15	5595
6D	8x12	7x12	7x12	3960
7D	7x10	6x10	6x11	2940
8D	6x9	5x9	6x9	2295
9D	5x8	5x8	5x8	1800
10D	5x7	4x7	5x7	1470
11D	4x6	4x7	4x7	1200
12D	4x6	4x6	4x6	1080
13D	4x6	3x6	4x6	930
14D	4x5	3x5	3x5	750
15D	3x5	3x5	3x5	675

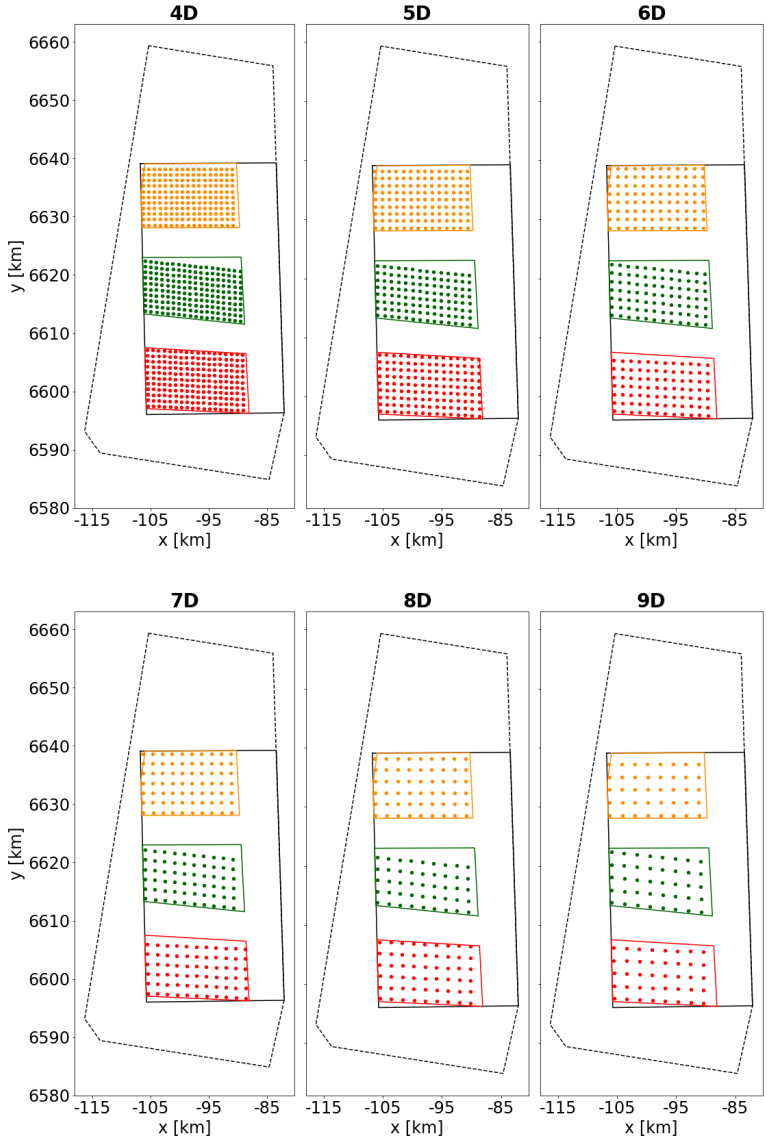

Figure 3.8: Wind Farm Layout with full area utilization of the designated project areas in Utsira Nord, using 4D-9D turbine distance

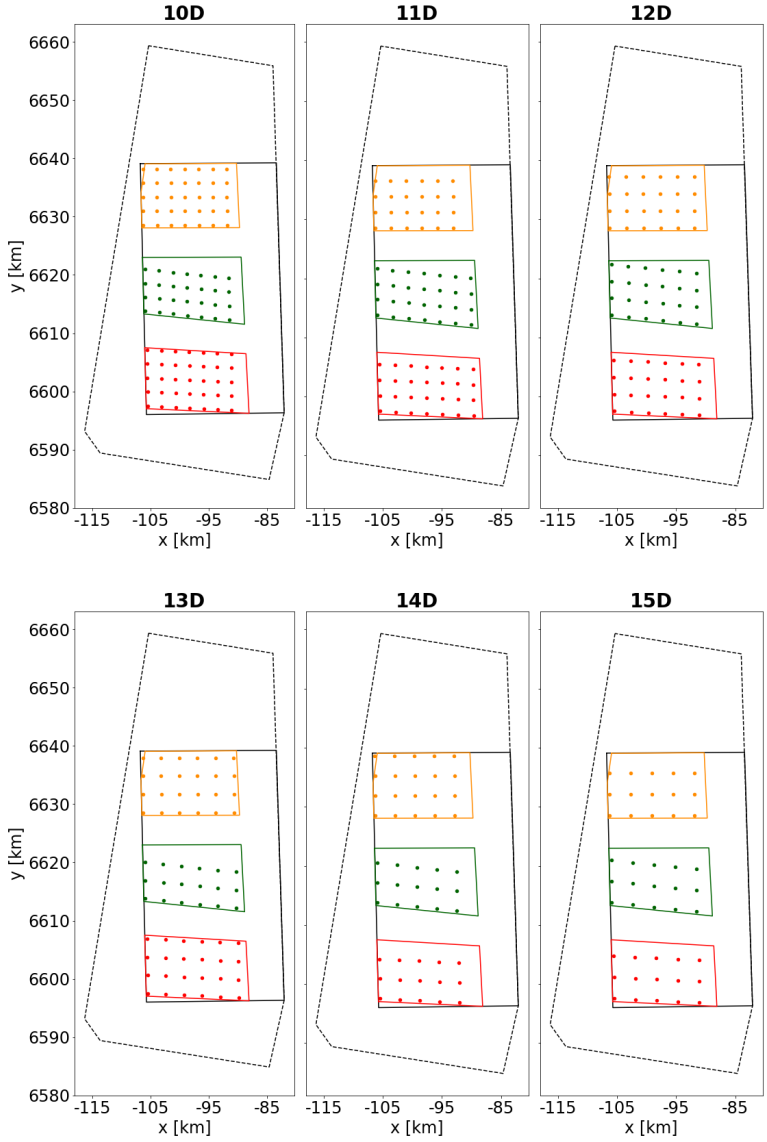

Figure 3.9: Wind Farm Layout with full area utilization of the designated project areas in Utsira Nord, using 10D-15D turbine distance

The wind farm designs for Utsira Nord as one uniform wind farm are listed in Table 3.4 for different turbine distances. As the wind farm is distributed over a larger area, the installed capacity is larger than for the corresponding turbine distances using the project areas. The installed capacity now range from 1260 MW for a turbine distance of 15D, which is 180 MW less than for the Initial Scenario, and 16200 MW for a turbine distance of 4D, more than five times the installed capacity of the Area Expansion Scenario. The wind farm layouts are illustrated in Fig. 3.10 and Fig. 3.11.

Table 3.4: Wind farm layouts and installed capacity for Utsira Nord without project areas

	Wind Farm Layout	**Installed Capacity [MW]**
4D	45x24	16 200
5D	36x20	10 800
6D	30x16	7 200
7D	26x14	5 460
8D	23x12	4 140
9D	20x11	3 300
10D	18x10	2 700
11D	17x9	2 295
12D	15x8	1 800
13D	14x8	1680
14D	13x7	1365
15D	12x7	1260

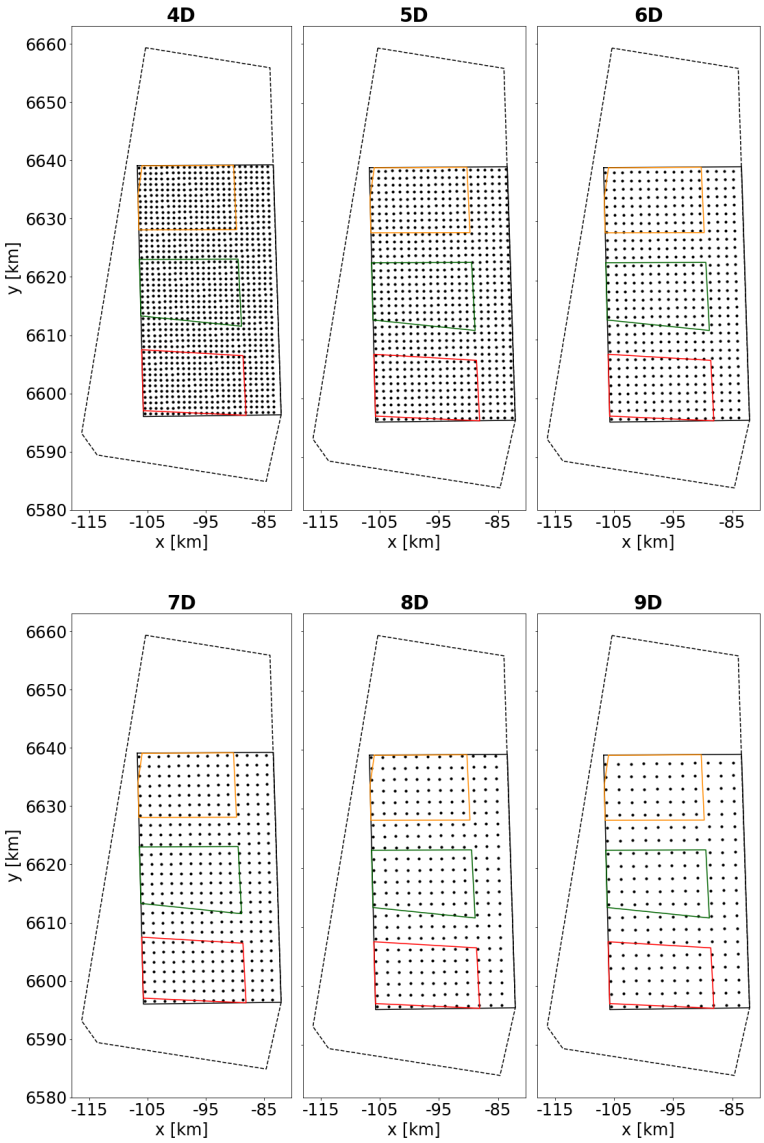

Figure 3.10: Wind farm layout for full area utilization of Utsira Nord without project areas, using 4D-9D turbine distances.

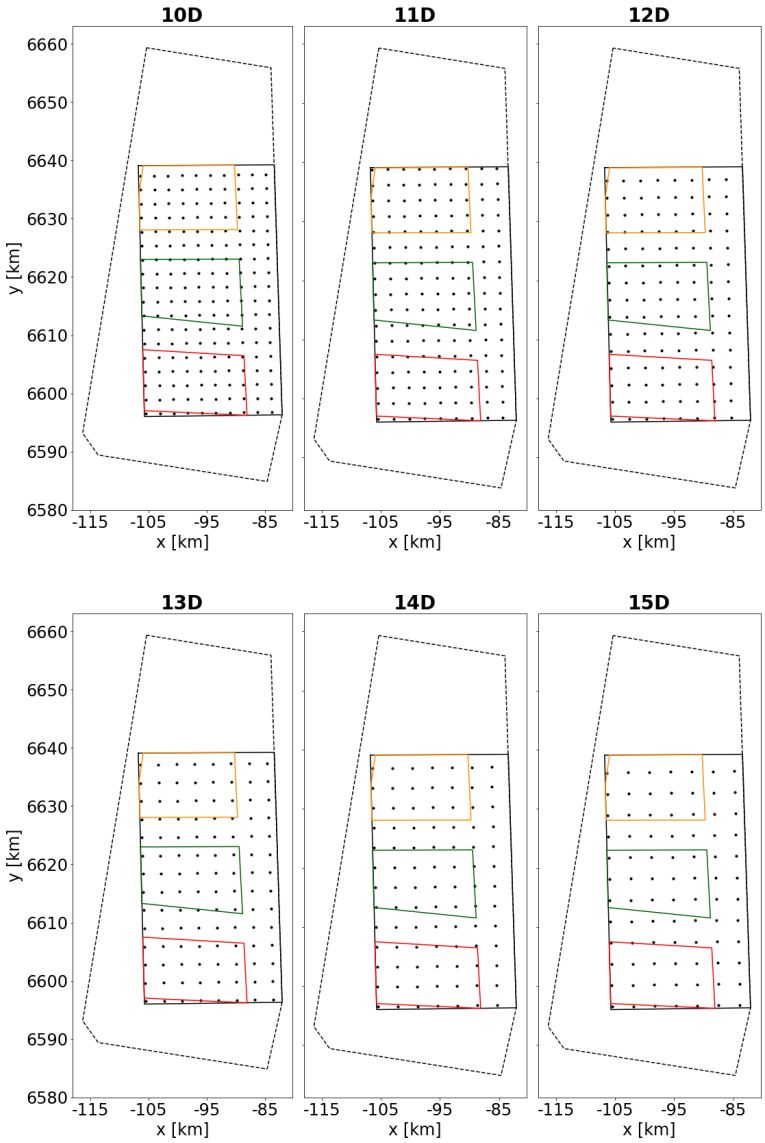

Figure 3.11: Wind farm layout for full area utilization of Utsira Nord without project areas, using 10D-15D turbine distances.

Chapter 4

Results

This chapter presents the results of wind farm modelling conducted at Utsira Nord and its expansion Vestavind F. Introductory, the wind conditions in the area are presented. Subsequently, the results of the two approaches described in section 1.1 are presented - first for the three scenarios of constant installed capacity from section 3.3.1 and finally for full area utilization as described in section 3.3.2.

4.1 Wind Conditions Utsira Nord

The wind rose for Utsira Nord at 150 meters hub-height, Fig. 4.1, show that there is a dominant wind from north-northwest and a secondary flow from south-southeast. There is minimal wind from the northeast to the east direction, between 45°-90°, while there is relatively consistent wind intensities from the southwest and the northwest direction, between 225°-315°. A more detailed presentation of the wind direction distribution is provided in Fig. 4.2. A wind direction of 346° is the most frequent over the 23 years.

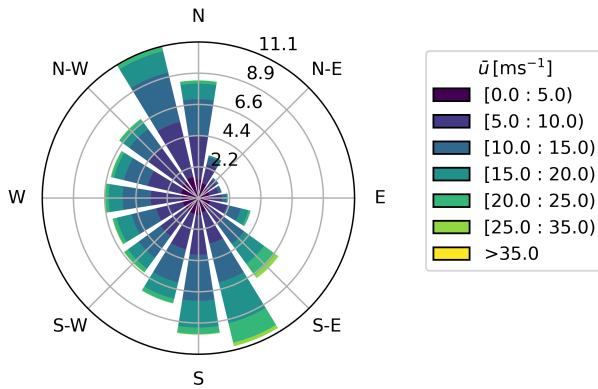

Figure 4.1: Wind rose for the Utsira Nord area from 2000-2022 at 150 m height with directional intervals of 22.5° and wind speed intervals of 5 m/s.

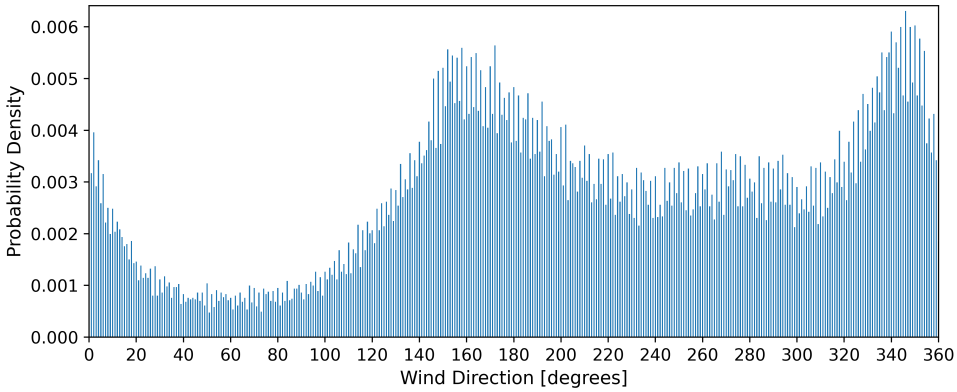

Figure 4.2: Distribution of wind direction occurence in Utsira Nord from 2000-2022 at 150 m height.

The mean wind speed is 10.5 m/s from 2000-2022, which is suitable for the IEA 15-MW turbine with a rated wind speed of 10.59 m/s. The corresponding mean turbulence intensity is calculated as 5.1% from the given wind speed and turbulent kinetic energy. By considering the production range of an IEA 15-MW wind turbine from 3-25 m/s, the average wind speed is 11 m/s, while the average turbulence intensity is 4.9%. The wind speed distribution at 150 meters hub-height and the corresponding power output for a single IEA 15-MW wind turbine is illustrated in Fig. 4.3. The wind speed distribution show a wind speed range up to 35 m/s. The corresponding distribution of power production reveal that the turbine produce no power about 8% of the time. This is mainly caused by occurrence of wind speeds that are lower than the cut-in wind speed of 3 m/s. From the graph, the turbine will run on rated power about 42% of the time. Thereby, the turbine runs at a partial load half of the time. These wind conditions enable a wind farm at Utsira Nord to produce an average 62% of its installed capacity over the designated time frame, without considering wake effects.

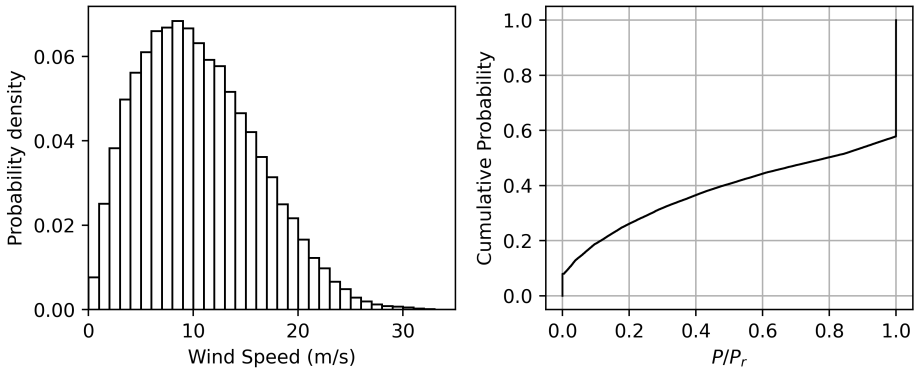

Figure 4.3: Distribution of wind speed (left) and the corresponding power production for a single IEA 15-MW turbine (right) in Utsira Nord from 2000-2022 at 150 m height.

Seasonal fluctuation of wind conditions are important to consider for accurate predictions of the wind farm performance. From Fig. 4.4 there is a larger density of higher wind speeds and turbulence intensities for January than July throughout the designated time frame, especially for wind speeds greater than 15 m/s. As the upstream wind speed have significant impact on the power production, this can cause greater production in January.

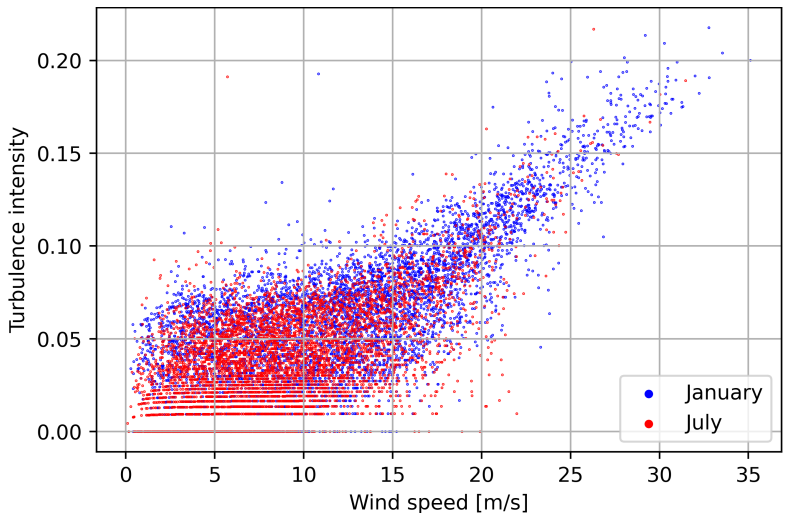

Figure 4.4: Turbulence intensity and wind speed for January and July from 2000-2022 at 150 m height.

There is a noticeable contrast in turbulence intensity for the summer and winter months in 2022, illustrated in Fig. 4.5. The occurrence of turbulence intensities over 4% is considerably smaller from May to September compared to the remaining months. From the statistics for wind speed and turbulence intensity in January and July from 2000-2022 presented in Table 4.1 for the wind speed range of 3-25 m/s, the mean turbulence intensity is 50% higher in January compared to July. The corresponding average wind speed is 25% higher.

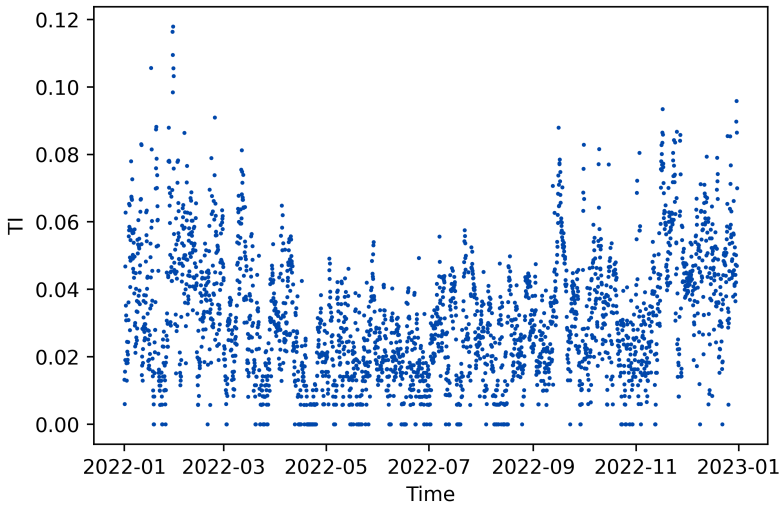

Figure 4.5: Turbulence intensity 2022 from NORA3 turbulence kinetic energy and wind speed data at 150 m height.

The three scenarios described in section 3.3.1 are used to compare wind farm power production using a constant 5% turbulence intensity against the turbulence intensity that is calculated for each data point from given turbulent kinetic energy and wind speed data, presented in Table 4.2. For the Initial Scenario, using a constant I_0=5% cause the farm production to be overestimated by 2 MW in July, compared to the calculated TI. The deviation increase with increasing installed capacity, causing an overestimation for both January and July of 1 MW and 3 MW respectively for the Capacity Expansion Scenario and 1 MW and 7 MW for the Area Expansion Scenario.

Table 4.1: Turbulence intensity and wind speed data within the production range of the IEA 15-MW wind turbine (U=3-25 m/s) from 2000-2022 at 150 m height.

	Turbulence Intensity [%]		**Wind Speed [m/s]**	
	January	July	January	July
Mean	6.3	4.2	12	9.6
Max	19	19	25	25
Min	0.0	0.0	3	3
Median	6.1	4.1	12	8.9

Table 4.2: Wind farm power production with wind data for January and July using calculated I_0 vs. I_0=5% for Scenario 1 (Initial Scenario), 2 (Capacity Expansion Scenario) and 3 (Area Expansion Scenario).

	Farm Power [MW]					
	Scenario 1		**Scenario 2**		**Scenario 3**	
	January	July	January	July	January	July
Calculated I_0	913	676	1405	1028	1868	1360
Constant I_0	913	678	1406	1031	1869	1367

The analysis of wind conditions in Utsira Nord at 150 m hub height reveals a dominant wind distribution from the north-northwest, with a secondary flow from the south-southeast, and minimal wind from the northeast to east. The average wind speed imply suitable conditions for the chosen IEA 15-MW wind turbine. Seasonal fluctuations with higher wind speeds and turbulence intensities in January compared to July affect wind farm performance, resulting in increased power production.

4.2 Approach 1: Constant Installed Capacity

This subsection present the wind power potential for Utsira Nord and Vestavind F with the wind farm layouts for Scenario 1 (Initial Scenario), 2 (Capacity Expansion Scenario) and 3 (Area Expansion Scenario) presented in 3.3.1. First, an analysis of the wind farm layouts with a turbine distance of seven rotor diameters (7D) is performed. The objective is to evaluate the consequence of increasing the installed capacity from comparison of the three scenarios, as well as investigating the effects and interactions of the defined project areas. Effects on wake loss both within each project area and from neighbouring project areas are investigated. This is performed by modelling each project area both with and without the others presence. Subsequently, a capacity density assessment is carried out by changing the turbine distance. Finally, the effects of using an alternative design that consider the dominant wind direction is investigated.

As mentioned in section 4.1, the average power output of a single IEA 15-MW wind turbine is 62% of its installed capacity without considering wake, with the given wind and turbine data. The resulting power produced from the wind farm without considering wake (Farm Ambient Power) for the three scenarios are listed in Table 4.3. For the individual project areas this corresponds to about 296 MW for the Initial Scenario and 463 MW for the Capacity Expansion and Area Expansion scenarios.

	Installed capacity [MW]	**Farm Ambient Power [MW]**
Scenario 1	1440	888
Scenario 2	2250	1388
Scenario 3	3000	1850

Table 4.3: Installed capacity and Farm Ambient Power for Scenario 1 (Initial Scenario), 2 (Capacity Expansion Scenario) and 3 (Area Expansion Scenario).

4.2.1 7D Turbine Distance

This subsection present the wind power potential for Scenario 1 (Initial Scenario), 2 (Capacity Expansion Scenario) and 3 (Area Expansion Scenario) in 3.3.1, using a 7D distance between the turbines. Two methods for increasing the installed capacity are presented. In the Capacity Expansion Scenario, the capacity is increased within the three existing project areas in Utsira Nord. In contrast, the Area Expansion Scenario have an additional project area with the same installed capacity as the Capacity Expansion Scenario for each area. These layouts constitute wind farm areas of 90 km^2 for each project area in the Initial Scenario and 141 km^2 for each project area in the Capacity Expansion and Area Expansion scenarios, which utilize 49% and 77% of the designated project areas respectively. The wake expansions for the wind farm layouts are illustrated in Fig. 4.6, from using a single state of mean wind conditions over the designated time frame. This visualization offer preliminary understanding of the resulting wake loss distribution for the turbines within the wind farms over the entire time period.

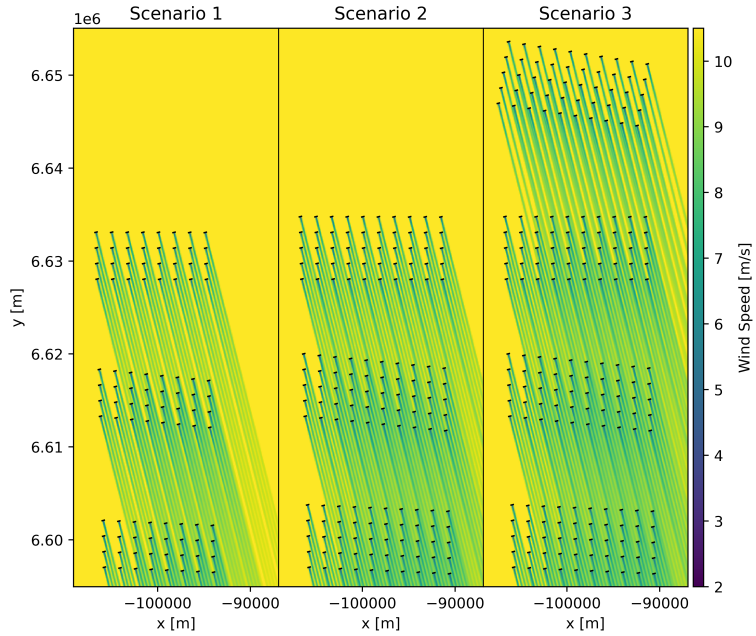

Figure 4.6: Wake plot for Scenario 1 (Initial Scenario), 2 (Capacity Expansion Scenario) and 3 (Area Expansion Scenario) with a 7D turbine distance using mean wind conditions of U=11 m/s, wd=346°, I_0=4.9%.

The wake loss of a wind turbine is very dependent on its placement in the wind farm. From Fig. 4.7 the turbines in the first row of the northernmost project area and the last row in the southernmost project area, as well as the turbines along the western boundaries of the wind farms, has the best conditions with the lowest average wake loss. The wake loss range from 2.7-10% per turbine for the Initial Scenario and 3.0-13% per turbine for the Capacity Expansion and Area Expansion scenarios. The turbines that experience most wake loss are in the middle rows, positioned slightly to the right of center in the wind farms. This is likely due to the dominant wind direction from north-northwest and south-southeast, stated in section 4.1. There are particularly high losses for wind farms that are surrounded by other project areas on both sides, caused by additional wake effects from neighbouring wind farms. The range of turbine wake loss reflects on the total wake loss for each scenario.

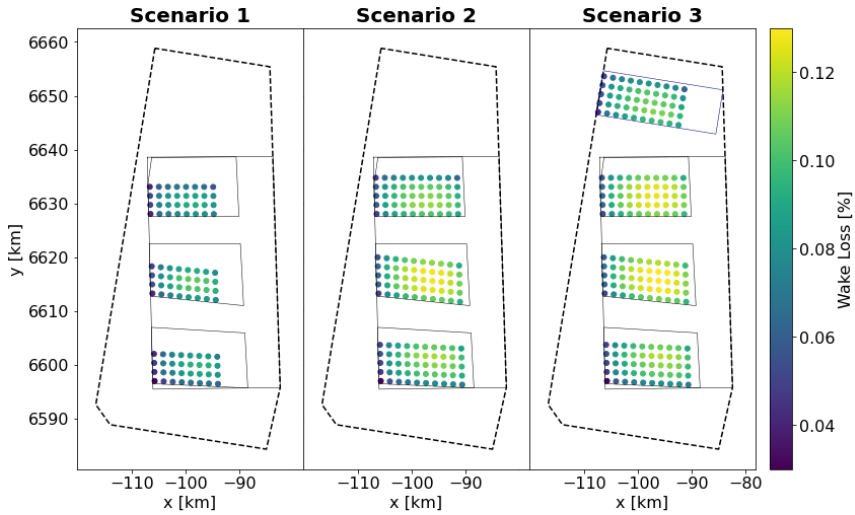

Figure 4.7: Average wake loss for each turbine in Scenario 1 (Initial Scenario), 2 (Capacity Expansion Scenario) and 3 (Area Expansion Scenario) with a 7D turbine distance from 2000-2022.

The capacity increase within each project area in the Capacity Expansion Scenario cause the power production to increase by 53% from the Initial Scenario, considering wake. The additional project area in the Area Expansion Scenario cause further power increase of 33% from the farm results listed in Table 4.4. The total wake loss is 7.7%, 9.5% and 9.8% for the three

scenarios respectively. Hence, increasing the installed capacity within the existing project areas increase the total wake loss by 1.8%, while adding an additional project area cause further wake loss of 0.3%. The additional wake loss from the two capacity expansions are caused by a combination of increased wake within each project area and increased wake from neighbouring project areas. Simulating each project area without the others presence reveals that the wake loss caused by turbines inside each area is 5.7% for the Initial Scenario with wind farms of 32 turbines and 7.0% for the Capacity Expansion Scenario and the Area Expansion Scenario with wind farms of 50 turbines. The remaining 2%, 2.5% and 2.8% for the three scenarios respectively from Table 4.4 is caused by wake effects from one project area to another. The following section explores how wind direction can influence wake loss.

Table 4.4: Wind Farm Results with all project areas present for Scenario 1 (Initial Scenario), 2 (Capacity Expansion Scenario) and 3 (Area Expansion Scenario), using a 7D turbine distance.

	Utsira Nord			
Project area	1	2	3	**Total**
Scenario 1				
Farm Power [MW]	274	271	275	820
Wake Loss [%]	7.4	8.4	7.2	7.7
Scenario 2				
Farm Power [MW]	420	414	421	1256
Wake Loss [%]	9.1	10.5	9.0	9.5
	Vestavind F			
Project area	1	2	3	4	**Total**
Scenario 3					
Farm Power [MW]	414	413	421	422	1669
Wake loss [%]	10.5	10.7	9.1	8.9	9.8

An assessment of the wind farm's sensitivity to wind directions is conducted using simulations with mean wind conditions and wind directions from 0°-359°. According to section 4.1, the mean wind conditions within the IEA 15-MW wind turbine's production range correspond to a wind speed of 11 m/s and a turbulence intensity of 4.9%. The resulting distribution of normalized wind farm power is illustrated in Fig. 4.8, where normalized power is the wind farm power divided by ambient power, indicating efficiency. The wake loss ranges from 2.1-53% for the Initial Scenario, 5.5-58% for the Capacity Expansion Scenario and 5.7-48% for the Area Expansion Scenario.

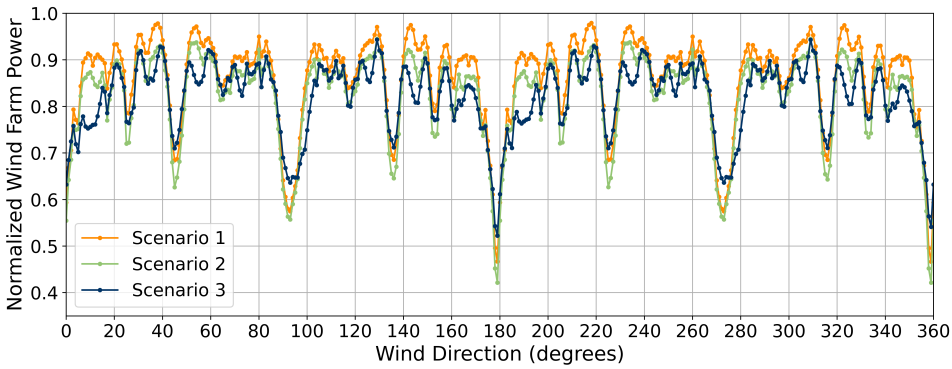

Figure 4.8: Distribution of the normalized wind farm power output for Scenario 1 (Initial Scenario), 2 (Capacity Expansion Scenario) and 3 (Area Expansion Scenario) obtained from single states of mean wind conditions of U=11 m/s and I_0=4.9% for wind directions from 0°-359°.

The wind direction causing the greatest wake loss is from north (359°) and south (179°), resulting in more than half of the power lost to wake. Specifically, a wind direction of 359° causes a wake loss of 53% for the Initial Scenario, 58% for the Capacity Expansion Scenario and 47% for the Area Expansion Scenario. The wake expansion for northerly winds is shown in Fig. 4.9. A prevailing wind direction of 346°, just 13° from 359°, reduces wake loss by half and doubles power production. For the Initial Scenario, wake loss decreases to 9.1% and power production increases by 212%. In the Capacity Expansion and Area Expansion scenarios, wake loss drops to 14% and 16%, respectively, increasing production by 205% and 155%. The wake expansion for 346° is illustrated in Fig. 4.6.

The wind directions causing the least wake loss differ across the three scenarios and is more evenly distributed for the various wind directions compared to the minima normalized power of maximum wake loss. For the Initial Scenario, minimal wake loss is 2.1%, while for the Capacity Expansion and Area Expansion scenarios, the minimal wake loss is 5.5% and 5.7% respectively.

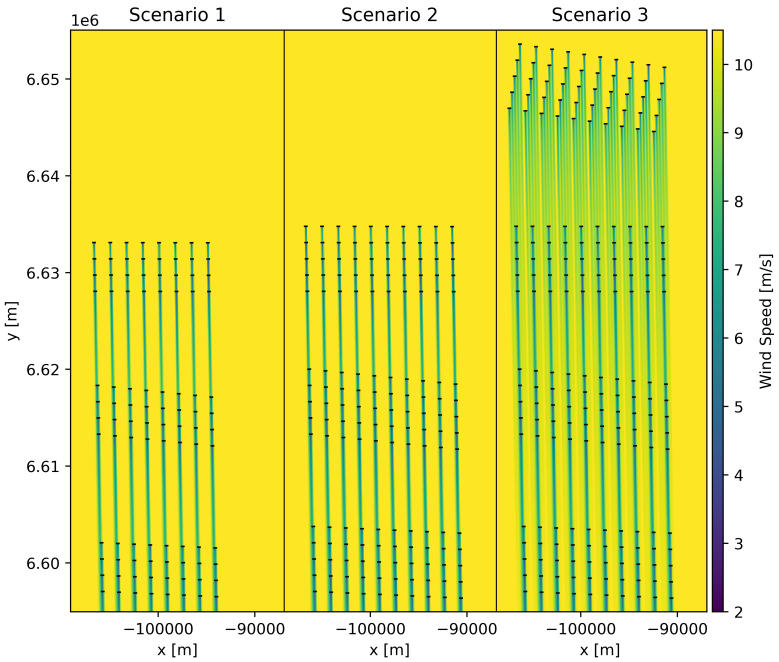

Figure 4.9: Wake Plot for Scenario 1 (Initial Scenario), 2 (Capacity Expansion Scenario) and 3 (Area Expansion Scenario) with a 7D turbine distance for U=11 m/s, wd=359°, I_0=4.9% for 2000-2022.

The results from this section reveal that increased capacity lead to higher wake losses, with varying effects on internal and external wake depending on the method of capacity expansion. Increasing the capacity within the project areas cause overall higher increase in wake loss compared to an additional project area, primarily due to a higher ratio of internal wake. Conversely, an additional project area does not affect internal wake significantly, resulting in lower increases in wake loss. In the final analysis, this chapter demonstrate the significant impact of wind direction on wind farm wake.

4.2.2 Capacity Density Assessment

This section aim to investigate the effects of capacity density on the wake loss by modelling the wind farms of Scenario 1 (Initial Scenario), 2 (Capacity Expansion Scenario) and 3 (Area Expansion Scenario) described in section 3.3.1 with different turbine distances. The results include turbine distances both within and outside announced capacity density range, including cases when the wind farms extends beyond the boundaries of the defined areas. From Table 4.5, the recommendation of 3.5-7.5 MW/km^2 with 33-100% area utilization limit the turbine distance to 6D-8D for the Initial Scenario and 6D-7D for the Capacity Expansion and Area Expansion scenarios. The area utilization is based on the stated area of 182 km^2 for each project area in Utsira Nord, with the corresponding area utilization of Utsira Nord (1010 km^2) and Vestavind F (1989 km^2) in the brackets. The utilization rate of Project Area 4 of Vestavind F in the Area Expansion Scenario is not included in the table as this area is not stated by the government.

Reducing the capacity density by increasing the turbine distance cause less wake loss and thereby improve the farm efficiency. A high farm efficiency imply a high capacity factor, which is defined as the ratio of the installed capacity that is actually produced. The effects of increasing the distance are greater for lower turbine distances, as illustrated for the farm efficiency in Fig. 4.10 and for the corresponding farm power production considering wake effects in Fig. 4.11. For a turbine distance of two rotor diameters, the wake loss reduces the power production by 19-22%. Increasing the turbine distance by one rotor diameters improve the farm efficiency significantly by 5%, resulting in a wake loss of 13-15% for 3D. This cause the production to increase by 42 MW, 71 MW and 94 MW for Scenario 1 (Initial Scenario), 2 (Capacity Expansion Scenario) and 3 (Area Expansion Scenario) respectively. In contrast, increasing the turbine distance from 13D to 14D increase the farm efficiency by 0.2-0.3%, with a corresponding production increase of 2-3 MW. The improvements from increasing the turbine distance is highly diminished as the distances become larger and the farm efficiencies are higher. To better understand the effects of capacity density, the ratio of internal and external wake with increasing turbine distance is examined.

Table 4.5: Wind farm area and capacity density for Scenario 1 (Initial Scenario), 2 (Capacity Expansion Scenario) and 3 (Area Expansion Scenario).

	Capacity density [MW/km^2]	**Utilization rate project areas** Scenario 1	Scenario 2	Scenario 3
2D	65	4% (2.2%)	6% (3.4%)	6% (2.3%)
3D	29	9% (4.9%)	14% (7.7%)	14% (5.2%)
4D	16	16% (8.75%)	25% (13.7%)	25% (9.3%)
5D	10	25% (13.7%)	40% (21.4%)	40% (14.5%)
6D	7.2	36% (19.7%)	57% (30.8%)	57% (20.85%)
7D	5.3	49% (26.8%)	77% (41.9%)	77% (28.4%)
8D	4.1	65% (35.0%)	101% (54.7%)	101% (37.1%)
9D	3.2	82% (44.3%)	128% (69.3%)	128% (46.9%)
10D	2.6	101% (54.7%)	158% (85.5%)	158% (57.9%)
11D	2.15	122.5% (66.2%)	191% (103.5%)	191% (70.1%)
12D	1.8	146% (78.8%)	228% (123%)	228% (83.4%)
13D	1.5	171% (92.5%)	267.5% (144.5%)	267.5% (97.9%)
14D	1.3	198% (107%)	310% (168%)	310% (113.5%)
15D	1.15	227% (123%)	356% (192%)	356% (130%)

() = utilization rate of Utsira Nord (1010 km^2) for Scenario 1 and 2, Vestavind F (1989 km^2) for Scenario 3.

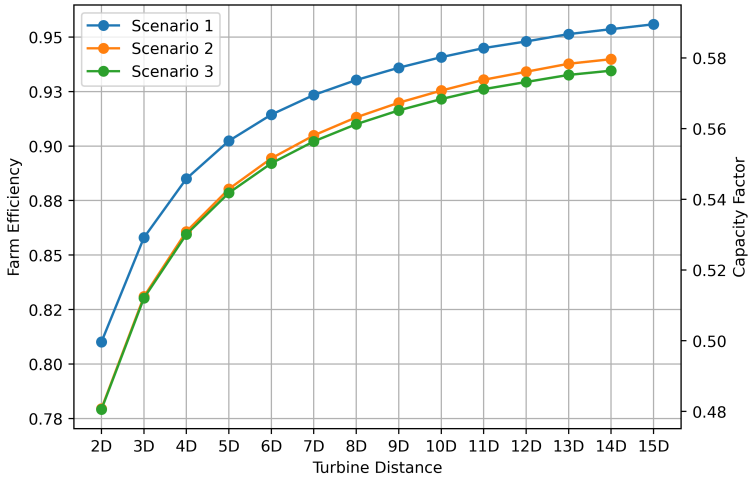

Figure 4.10: Farm efficiency and capacity factor with increasing turbine distance for Scenario 1 (Initial Scenario), 2 (Capacity Expansion Scenario) and 3 (Area Expansion Scenario).

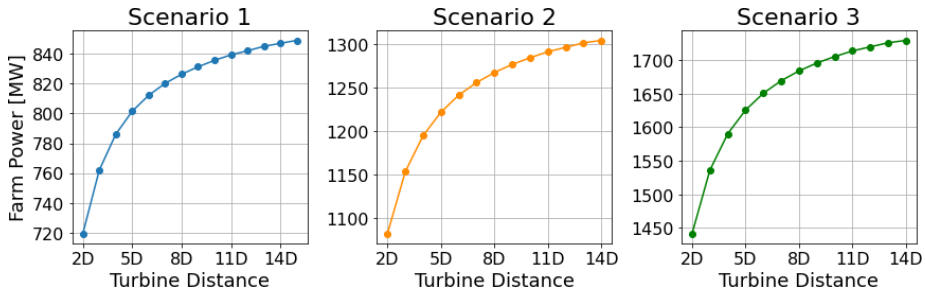

Figure 4.11: Farm power with increasing turbine distance for Scenario 1 (Initial Scenario), 2 (Capacity Expansion Scenario) and 3 (Area Expansion Scenario).

The capacity density analysis is continued by studying the distribution of internal and external wake. From Fig. 4.12 there is a strong majority of internal wake loss for the lower turbine distances, as there is little distance between the turbines within each wind farm while there is larger distance and thereby less wake effects from neighbouring wind farms. As the distance between each turbine increase, so does the wind farm size, causing less distance between the wind farms of each project area. Thereby, the external

wake losses increase with increasing turbine distances while internal wake loss decrease. The reduction of internal wake loss outweighs the increase in external wake loss, resulting in an overall decrease in total wake losses. These results allow for further investigation of how the capacity expansions affect the wake loss, by comparing the three scenarios.

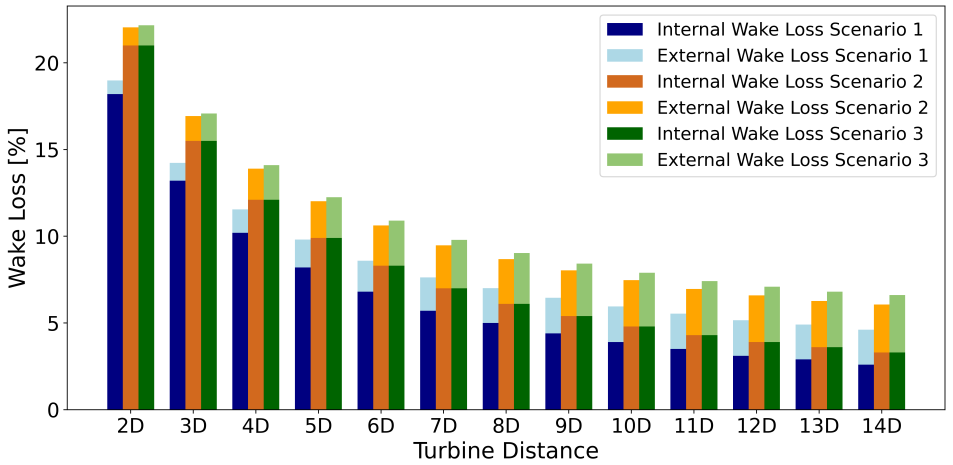

Figure 4.12: Ratio between internal wake loss within each project area and external wake loss between project areas for Scenario 1 (Initial Scenario), 2 (Capacity Expansion Scenario) and 3 (Area Expansion Scenario) with increasing turbine distance.

The additional wake loss from increasing the number of turbines for each project area in the Capacity Expansion Scenario are most significant for shorter turbine distances, when the internal wake loss is dominant. As the turbine distance increase and there is a more even distribution of internal and external wake loss, the deviations between the Initial Scenario and the Capacity Expansion Scenario decreases. The contrary effect is observed for adding a fourth project area in the Area Expansion Scenario. For smaller turbine distances, there are minimal difference in wake loss from the three comparable project areas in the Capacity Expansion Scenario. As the turbine distance grows, the internal wake loss remains equivalent due to an equal amount of turbines in the wind farms of each project area. Simultaneously, the external wake loss grows larger for the Area Expansion Scenario than the Capacity Expansion Scenario because of wake from the additional project

area. Hence, the overall increase in wake loss is smaller from adding a fourth area compared to increasing the capacity within each project area for all turbine distances.

In summary, the capacity density analysis for the three scenarios reveal overall reduced wake loss for increasing turbine distance. However, the wind farm layouts in the Capacity Expansion and Area Expansion scenarios exceed the designated project areas for turbine distances of 8D and more, and similarly for 10D and more in the Initial Scenario. The wind farm areas expand with growing distance between the turbines, which cause reduced internal wake and increasing external wake for increasing turbine distance in all scenarios.

4.2.3 Alternative Wind Farm Layout

This section explores the impact on wake effects from considering the prevailing wind direction when determining turbine spacing in the wind farms of Scenario 1 (Initial Scenario), 2 (Capacity Expansion Scenario) and 3 (Area Expansion Scenario) that is described in section 3.3.1. The orientation of the turbine rows is kept unchanged while the turbine distance is adapted to the dominant wind by using 5D within the turbine rows and 9D between them. These layouts utilize 46% and 71% of the project areas and 25 and 38% of Utsira Nord for the Initial Scenario and the Capacity Expansion Scenario respectively. The alternative layout for the Area Expansion Scenario use 26% of Vestavind F. The wake expansions for the alternative layouts are visualised in Fig. 4.13, using mean wind conditions for the production range of the IEA 15-MW turbine from 2000-2022. This visualization provides initial insight into the resulting wake loss distribution within the wind farms over the entire time period.

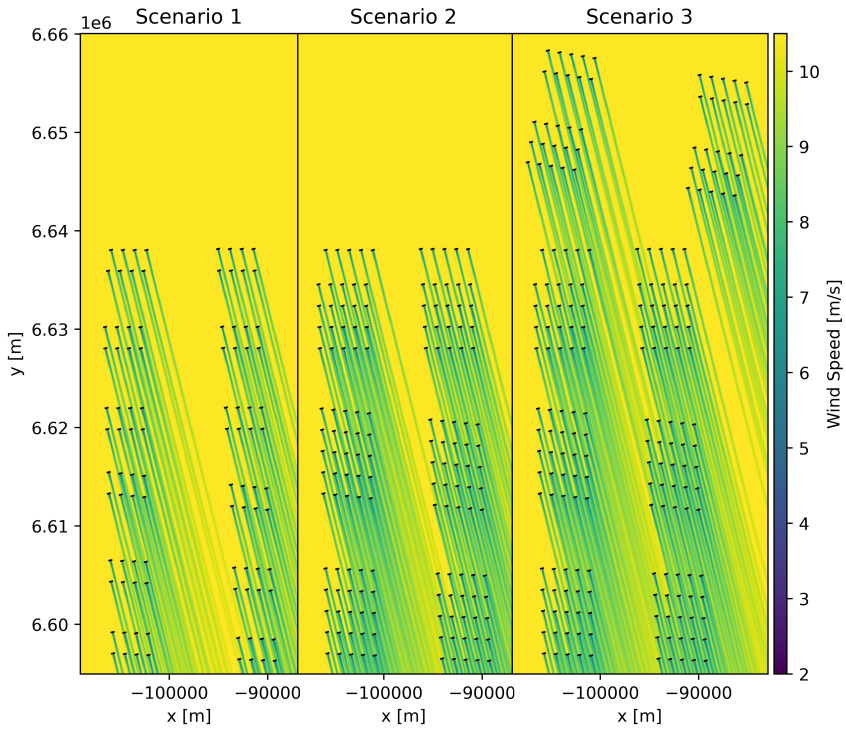

Figure 4.13: Wake plot for Scenario 1 (Initial Scenario), 2 (Capacity Expansion Scenario) and 3 (Area Expansion Scenario) with alternative layout using 5D within each turbine row and 9D between them, using mean wind conditions of U=10.5 m/s, wd=346°, I_0=4.9%.

The alternative wind farm layout show different wake loss patterns within the wind farms. The resulting wake loss for each turbine is illustrated in Fig. 4.14 for each scenario. Separating the wind farms into clusters reduce the number of turbines placed in the centre of the wind farms that normally experience most wake. For the Initial Scenario, with clusters of only two rows each, there are no centre turbines. All three project areas are designed by placing the clusters in each corner of the area, maximizing the distance between them. The resulting turbine wake loss range from 2-9%. For the Capacity Expansion and Area Expansion scenarios there is not enough available space for four clusters in the three project areas of Utsira Nord with the chosen turbine distance. This result in more centre turbines compared to the Initial Scenario. The fourth project area in the Area Expansion Scenario is not predefined by the government, but is chosen to expand along the

upper borders of Vestavind F here. This constitutes a large enough area to divide the wind farm into four clusters. The wake loss for the turbines in this project area is reduced compared to the northernmost project area in the Capacity Expansion Scenario, which imply good effects from the additional clustering. The range of turbine wake for the Capacity Expansion and Area Expansion scenarios is 3-12%. The contrasts in turbine wake loss for the three scenarios reflects on the corresponding wake loss for the whole wind farms.

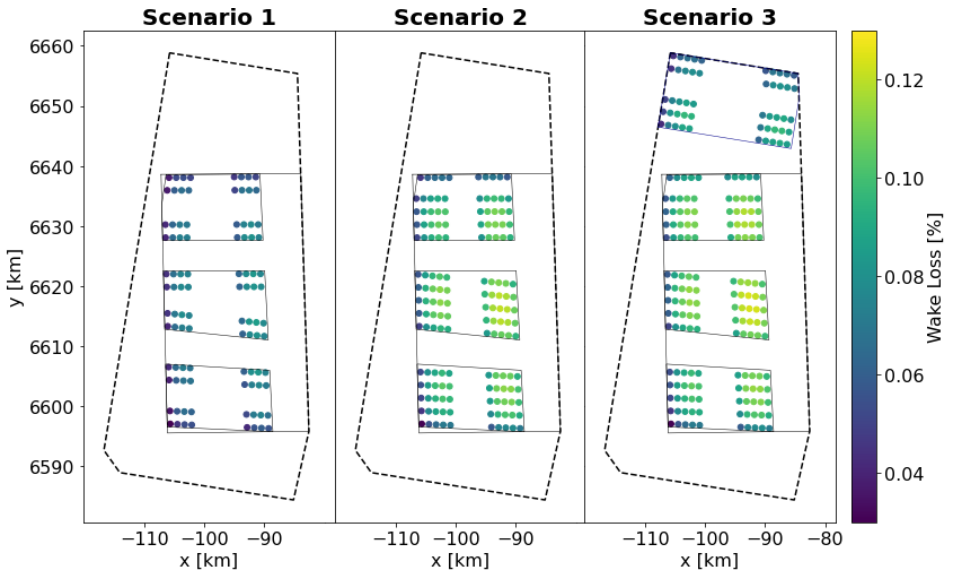

Figure 4.14: Average wake loss for each wind turbine in Scenario 1 (Initial Scenario), 2 (Capacity Expansion Scenario) and 3 (Area Expansion Scenario) with alternative layout using 5D within each turbine row and 9D between them, from 2000-2022.

The wind farm productions and the corresponding wake losses with the alternative wind farm layouts are listed in Table 4.6. The total wake loss is 6.4% for the Initial Scenario of four clusters in each project area and 9.0% for both the Capacity Expansion and the Area Expansion Scenario. To better understand how the wind farm layouts affect the resulting wake losses, the ratio of internal and external wake is examined.

Table 4.6: Wind farm results for Scenario 1 (Initial Scenario), 2 (Capacity Expansion Scenario) and 3 (Area Expansion Scenario) with alternative wind farm layout of 5D within each turbine row and 9D between them, with all project areas present.

	Utsira Nord			
Project area	1	2	3	**Total**
Scenario 1				
Farm Power [MW]	278	275	278	831
Wake Loss [%]	6.1	7.0	6.0	6.4
Scenario 2				
Power [MW]	423	417	423	1263
Wake Loss [%]	8.6	9.9	8.6	9.0

	Vestavind F				
Project area	1	2	3	4	**Total**
Scenario 3					
Farm Power [MW]	418	415	422	428	1684
Wake loss [%]	9.6	10.2	8.7	7.5	9.0

Internal wake loss is still defined as the wake loss within each project area, not within each cluster. Correspondingly, external wake loss is from neighbouring project areas. For the Initial Scenario, 70% of the total wake loss is internal, constituting 4.5% internal and 1.9% external wake loss. The wake loss for the Capacity Expansion Scenario is 75% internal, specifically 6.7% internal and 2.3% external wake. The ratio of internal and external wake in the Area Expansion Scenario differ from the Capacity Expansion Scenario with less internal and more external wake loss. To be specific, the total wake loss of the alternative layout in the Area Expansion Scenario is 72% internal, constituting 6.5% internal and 2.5% external wake loss. More external wake loss is expected as the results from section 4.2.2 showed additional wake from the added fourth project area. The decreasing ratio of internal wake loss implies that the wind farm layout of the extra project area

in the Area Expansion Scenario has greater improvement for internal wake loss compared to the remaining areas. These results may also be connected to the more angled layout of the fourth project area, as upcoming results will demonstrate the significant impact of wind direction on wake loss.

By simulating the alternative layout for single states of mean wind conditions of 11 m/s and 4.9% turbulence intensity with wind directions from 0°-359°, the distribution of the normalized wind power output is obtained for the alternative layouts, visualized in Fig. 4.15. The normalized wind farm power represent the ratio of wind farm production considering wake effects to the power production without wake effects, thus reflecting the wind farm efficiency. The wake loss for these parameters range from 0.7-44.3% for the Initial Scenario, 5.6-48.8% for the Capacity Expansion Scenario and 5.3-42.7% for the Area Expansion Scenario. For the dominant wind direction of 346°, the wake loss is 9.4%, 14.8% and 15.2% for the three scenarios respectively.

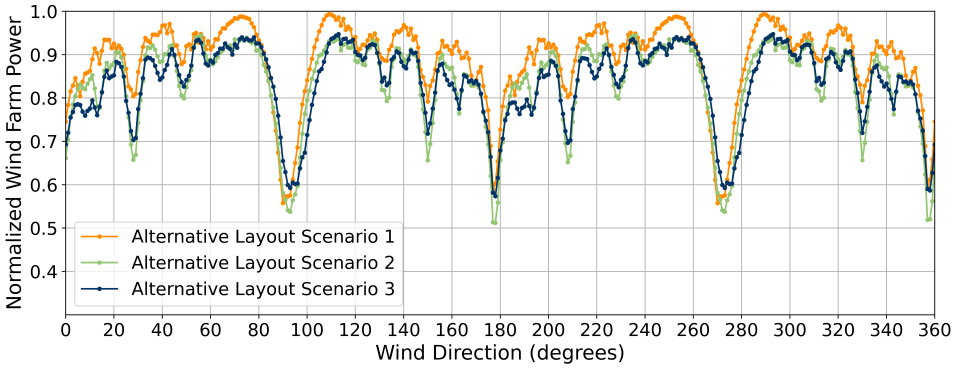

Figure 4.15: Distribution of normalized wind farm power for Scenario 1 (Initial Scenario), 2 (Capacity Expansion Scenario) and 3 (Area Expansion Scenario) with alternative layout using 5D within each turbine row and 9D between them, obtained from single states of mean wind conditions of U=10.5 m/s and I_0=4.9% for wind directions from 0°-359°.

The results from investigating the wake effects for alternative layouts that consider the prevailing wind direction imply that both installed capacity and wind farm design have significant impact on the resulting wake losses. The Initial Scenario, with the lowest installed capacity and the possibility of

four clusters, show the least wake loss. The capacity increase require larger wind farm area, which limit the division of wind farms into two clusters in the east-west direction, except for Project Area 4 where the area is not yet defined by the government. The turbine wake loss for the three scenarios show noticeable effects on wake loss from reducing central turbines and division into four clusters instead of two. Lastly, the significant influence of the wind direction on the wake loss and resulting power production is evident.

4.3 Approach 2: Full Area Utilization of Utsira Nord

This section explore the effect of full area utilization in Utsira Nord with and without project areas. The resulting installed capacities and the corresponding wind farm power productions are illustrated in Fig. 4.16. Larger turbine spacing require less turbines, causing a lower installed capacity. Full utilization of Utsira Nord with project areas results in a production range from 404 MW for a 15D turbine distance to 4057 MW for 4D. By using all of Utsira Nord without project areas, the available area is increased by 85% from 546 km^2 for all three project areas to 1010 km^2 for Utsira Nord. As the utilization rate of the designated areas depend on the turbine distance, the growth in wind farm size range from 67-98%. The corresponding farm power increases by 64-84%, dependent on the turbine distance, with a power production range of 745-5197 MW from using the whole area. To make a comprehensive assessment of the consequences from using the whole uniform area instead of separating it into three smaller project areas, the impact on wake loss is essential.

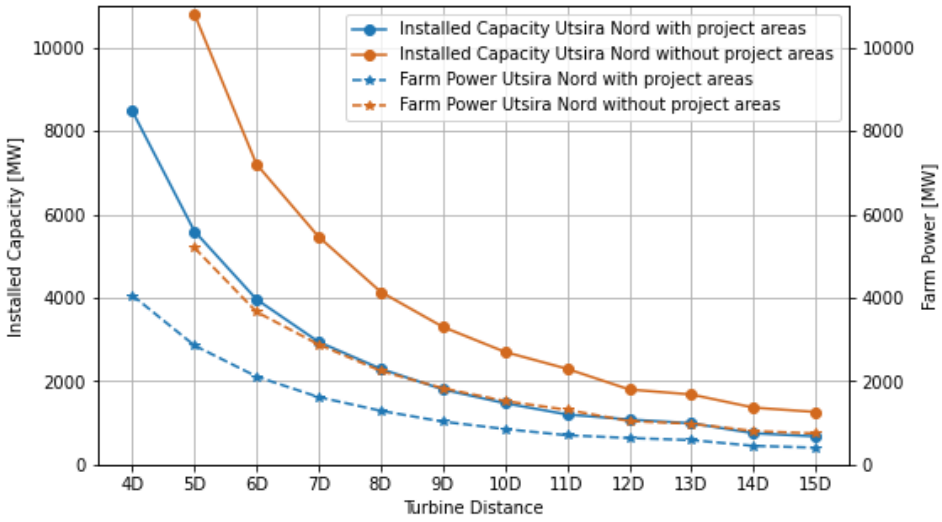

Figure 4.16: Installed capacity and the power production considering wake loss for wind farms with full area utilization in Utsira Nord with and without project areas

From Fig. 4.17 the increased power production from using the whole area of Utsira Nord also implies greater wake loss and hence lower farm efficiency. Lower farm efficiency also entails lower capacity factor. The wake loss for full area utilization of Utsira Nord with project areas range from 2.9% for a 15D turbine distance to 22% for a 4D turbine distance. Full area utilization of Utsira Nord as a uniform wind farm range from 4% for a turbine distance of 15D to 22% for a turbine distance of 5D. The increased wake loss from Utsira Nord as a uniform wind farm compared to using project areas is larger for shorter turbine distances, showing a 5% increase in wake loss for a turbine distance of 5D, specifically 17% wake loss with project areas and 22% without. For a turbine distance of 15D the difference is reduced to 1.3%. The wake loss is now only 2.9% with and 4.2% without project areas. To better understand how the wind farm area expansion affect the resulting wake losses, the ratio of internal and external wake is examined.

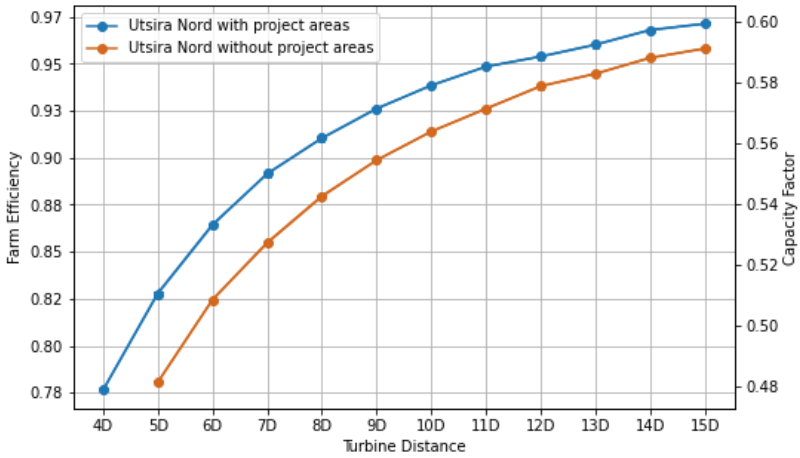

Figure 4.17: Farm efficiency and capacity factor for wind farms with full area utilization in Utsira Nord with and without project areas

Ratio of internal and external wake loss for increasing turbine distance is shown in Fig. 4.18. Utsira Nord as a uniform wind farm has only internal wake losses. With project areas, internal wake dominates, especially for lower turbine distances. Both internal and external wake effects decrease with growing turbine distance. The reduction of internal wake loss is more significant, resulting in an increasing ratio of external wake loss.

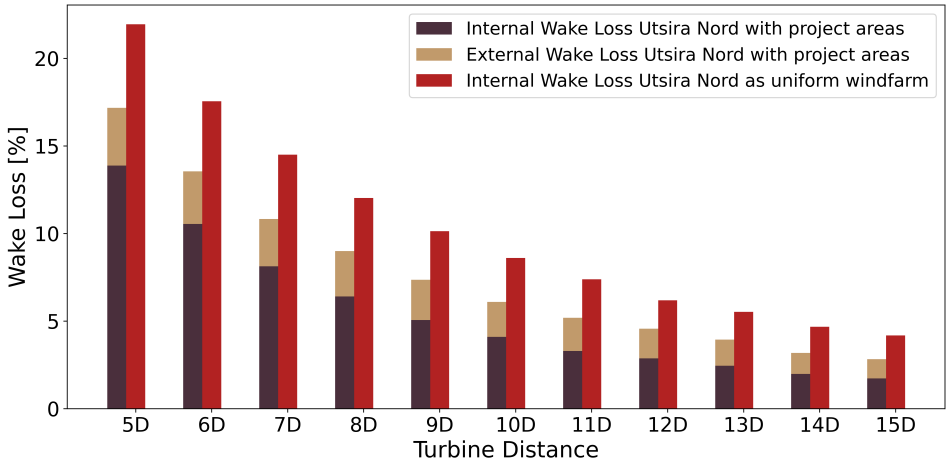

Figure 4.18: Internal and external wake loss using full area utilization in Utsira Nord with and without project areas.

Comparing two cases with the same installed capacity imply that the uniform area cause less wake loss and thereby higher farm efficiency. An 8D turbine distance with project areas correspond to the same installed capacity as using a 11D turbine distance for the whole area as a uniform wind farm. The distribution of wake loss in the wind farms are illustrated in Fig. 4.19. There are more internal wake loss for the uniform wind farm, but the total wake loss is larger for the three project areas with shorter turbine distance. The total wake loss is 7.4% without project areas, corresponding to a power production of 1311 MW. With project areas, the total wake loss is 8.95%, where 6.4% is internal wake. This constitute a power production of 1289 MW. Hence, utilizing the whole area of Utsira Nord allow for more distance between each turbine and reduces the wake loss by 1.55%, corresponding to 22 MW, while requiring an additional area of 464 km^2. In contrast, comparing the two wind farm layouts using the same turbine distance will cause more wake loss for the uniform wind farm due to more turbines.

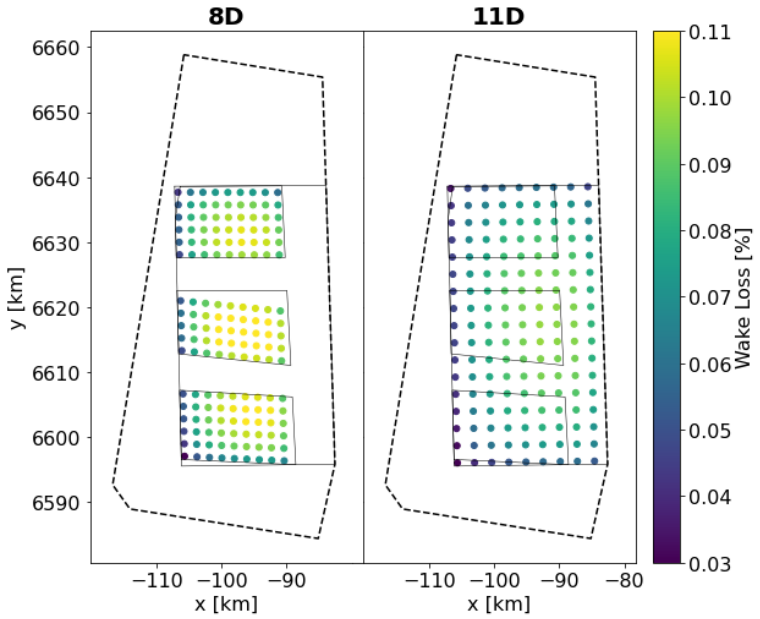

Figure 4.19: Turbine wake loss for 2295 MW installed capacity from full area utilization of Utsira Nord with project areas (8D turbine distance) and without project areas (11D turbine distance).

For a 7D turbine distance, a uniform wind farm produce 2877 MW while a wind farm within the three project areas produce 1616 MW. However, the uniform layout implies greater wake loss of 15%, compared to 11% with project areas. A uniform wind farm have more turbines placed in the centre of the wind farm. These turbines experience more wake loss, as illustrated in Fig. 4.20 of the turbine wake loss using a turbine distance of 7D. To summarize, there is a 78% greater production for Utsira Nord as a uniform wind farm and consequently 4% more wake loss, compared to using the designated project areas with a 7D turbine distance.

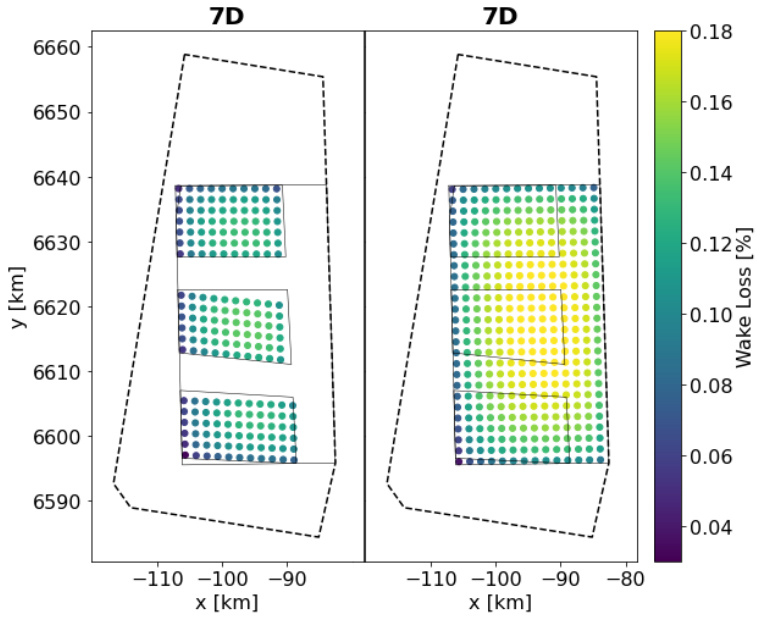

Figure 4.20: Turbine wake loss with full area utilization of Utsira Nord with and without project areas, using a 7D turbine distance.

The second approach with full area utilization of Utsira Nord with and without considering project areas show that the area as a uniform wind farm offer potential for significant capacity expansion compared to using the three government defined project areas. However, this capacity expansion also induce greater wake loss for the same turbine distances, as there are more turbines to generate wake and more turbines placed in the centre of the wind farm that experience more wake effects. In contrast, for a given installed capacity the uniform area allow for greater distance between the turbines and induce less wake loss compared to the project areas.

Chapter 5

Discussion

This chapter presents results from the two approaches employed in this study, comparing the outcome for different solutions of wind farm layouts in the area of Utsira Nord. The objective of these comparisons is to evaluate the effects of different wind farm design parameters such as installed capacity and turbine distance, in addition to highlight the effect of wind conditions such as turbulence intensity and wind direction on the wind farm wake loss. Comparison of a constant turbine distance with an alternative wind farm layout that consider the prevailing wind direction reveals how accounting for wind direction in turbine spacing can impact the wind farm performance. Lastly, the offshore wind power potential for the Utsira Nord area that results from these simulations are presented.

5.1 Importance of Turbulence Intensity

From section 4.1, the common practice of using a constant turbulence intensity overestimate the wind farm power with 7 MW for July compared to using calculated turbulence intensity from given wind data with the layout in the Area Expansion Scenario, which corresponds to a monthly overestimation of 5.1 GWh. The overestimation is enough energy to provide for more than 4000 households for a month, assuming a yearly consumption of 15 MWh from published statistics from 2022 by Ann Christin Bøeng, Statistisk sentralbyrå (SSB) (2023). Further statements of annual energy production is based on this assumption. The overestimations are shown to increase with increasing installed capacity from comparing Scenario 1 (Initial Scenario), 2 (Capacity Expansion Scenario) and 3 (Area Expansion Scenario). Thereby, the overestimation can be expected to be more significant for wind farms larger than the ones presented in these scenarios.

Increased turbulence intensity contribute to faster wake recovery and is expected to benefit the farm efficiency. Hence, a mean turbulence intensity

of 6.3% in January is expected to cause greater power production than using a constant 5% value. However, a constant I_0 predict greater power production for both months. This can be explained by the fact that the resulting power production from the wind farm simulations is only affected by turbulence intensity for wind speeds that are below rated wind speeds, with the wake model TurbOPark. This is shown from the power distribution as a function of wind speed, with the corresponding average turbulence intensity in Fig. 5.1. The calculated I_0 show values under 5% for wind speeds below 12 m/s, which cause the wind farm power production to be slightly lower in this range than for a constant 5% TI.

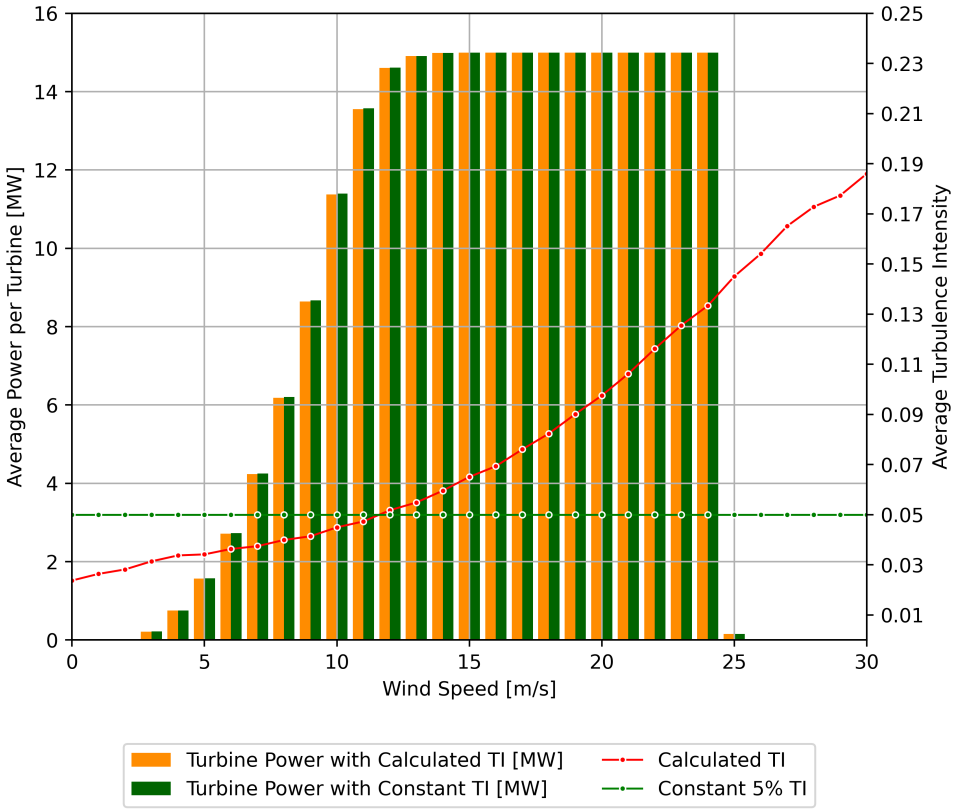

Figure 5.1: Distribution of power per turbine as a function of wind speed using calculated I_0 versus constant 5% I_0. Simulations are carried out by simulating the wind farm in the Initial Scenario with a 7D turbine distance, considering wake effects.

5.2 Importance of Wind Direction

The wind direction is an important consideration for optimal wind farm design, as it effects the available distance for a turbine wake to recover before encountering other wind turbines. The wind farm performance is shown to be very sensitive to the direction of the incoming wind for wind farm layouts of constant turbine distances in Fig. 4.15. The simulations are carried out using mean wind conditions of 11 m/s wind speed and 4.9% turbulence intensity. The resulting wake loss range from 48-58% for the worst situations to 1-6% for the best, dependent on the wind farm layout. Relative small changes in wind direction of 13° can cause the wake loss to be reduced by half. The dominant wake direction from north-northwest (346°) is shown to be neither the best nor the worst wind direction for minimal wake loss for the given wind farm layouts. This wind direction cause a wake loss of 9.1%, 14% and 16% for Scenario 1 (Initial Scenario), 2 (Capacity Expansion Scenario) and 3 (Area Expansion Scenario) respectively for single states of the mean wind conditions of 11 m/s and 4.9% turbulence intensity. As the wind farm layouts in these scenarios are based on the borders of the government defined project areas, these results imply that the angle of the future wind farms in these areas could benefit from considering the prevailing wind directions instead of following the area borders.

Comparison of a constant 7D turbine distance and an alternative layout of 5D within the turbine rows and 9D between them, show that the wind farm layout can have significant effects on the wind direction sensitivity. The farm power as a function of wind direction with a 7D turbine distance in Fig. 4.8 show two strong minima around 179° and 359° that cause significantly more wake loss compared to other wind directions, with a range of 48-58% that depend on the scenario. From the distribution of wind directions in the given area, illustrated in Fig. 4.2, these wind directions are quite frequent over the 23 year period. The alternative layout decrease the depths of these minima, so that the maximum wake loss is reduced by 9.1% for the Initial Scenario and the Capacity Expansion Scenario, and 5.1% for the Area Expansion Scenario. Now, there are four dominant minima with maximum wake loss of 43-50% for wind directions of 179°, 359°, 90° and 270°. These wind directions occur less frequently (Fig. 4.2). The improvement for minimal wake loss is best for the alternative layout in the Initial

Scenario, with a reduction of 1.4%, from 2.1% for a 7D distance to 0.7% for the alternative layout. These results show that wind farm layout affect the range of wake loss for different wind directions, with more pronounced impact on maximum wake loss, as well as it affects what wind directions that cause most and least wake. This show that knowledge about the wind direction distribution in the wind farm area is an important parameter in wind farm design, to ensure minimal wake effects for the most frequent wind directions.

5.3 Effect of Capacity Increase

Comparison of the three scenarios of different installed capacities with a constant 7D turbine distance provide insight into the effects of capacity expansion on the wake loss, and thereby the wind farm efficiency. The additional wake loss from increasing the capacity within each project area from the Initial Scenario to the Capacity Expansion Scenario is mainly caused by wake effects within each project area. From the 1.8% additional wake loss, 1.3% is caused internally. The remaining 0.5% is caused by increased wake from neighbouring wind farms as the distance between them decrease with the additional turbine row in each area. The capacity increase from adding a fourth project area while remaining the number of turbines within each project area constitute a much smaller wake loss addition, from comparing the Capacity Expansion Scenario and the Area Expansion Scenario. The internal wake loss is the same for both scenarios, while the additional project area in the Area Expansion Scenario cause the external wake loss to increase by 0.3%. Project area 1 is most affected as it now have an additional neighbouring project area in the northerly direction, while there is less change for the two remaining areas of Utsira Nord. These results imply that adding a new project area cause less consequences for the wind farm efficiency, as the external wake effects are less significant than the dominating internal wake, which will remain constant as the number of turbines for each project area remain the same.

Further capacity increase is investigated using the second approach, first with full utilization of the three project areas in Utsira Nord. From Fig. 5.2 that combine results on wake loss and corresponding farm power productions

for a constant turbine distance (section 4.2.2) and for full area utilization (section 4.3), a turbine distance less than 9D is required to achieve capacity expansion from full utilization of the project areas, compared to the Capacity Expansion Scenario of 2250 MW in the same area. Placing the turbines further than 9D apart results in less power produced with corresponding less wake effects. Full area utilization with a turbine distance of 7D produce 29% more power than the Capacity Expansion Scenario with the same turbine distance, which entails 1.6% additional wake loss. The wind farm of the Capacity Expansion Scenario will exceed the project areas for turbine distances of 8D and more, and will gradually resemble a uniform wind farm as the turbine distances grow and the distance between each project area diminish.

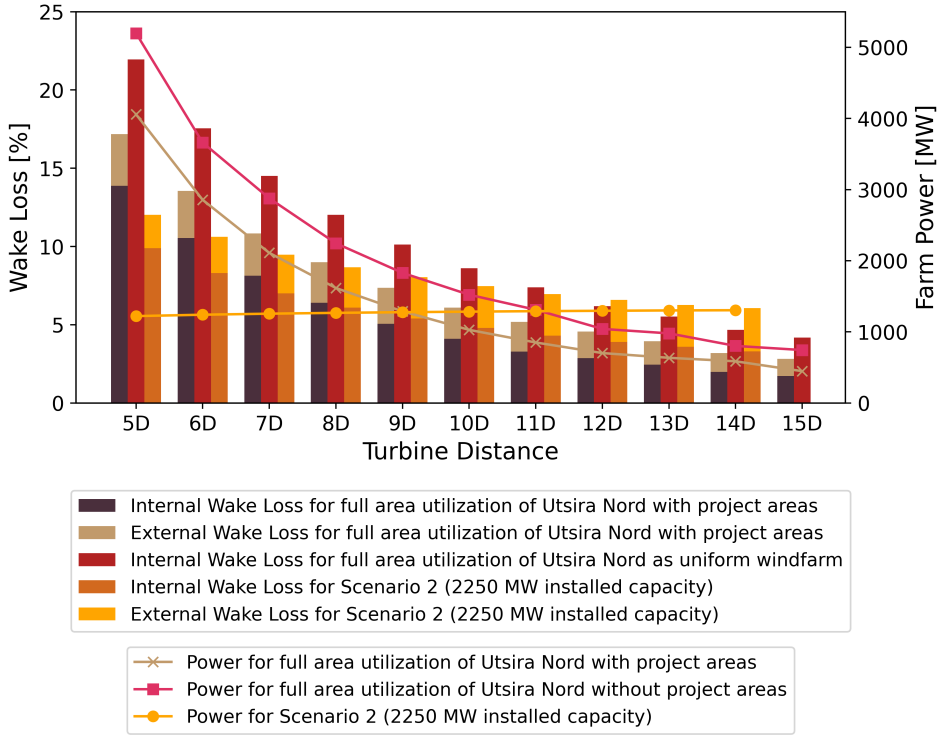

Figure 5.2: Wake loss and farm power production with increasing turbine distance for Utsira Nord with and without project areas compared to the Area Expansion Scenario with constant installed capacity of 3000 MW.

Full utilization of Utsira Nord without considering project areas allow for more power production than full area utilization with project areas. The uniform wind farm also produce more power than the Capacity Expansion Scenario when placing the turbines within 11 rotor diameters. For a 11D turbine distance, the respective wind farm productions are almost equivalent, illustrated in Fig. 5.2. The 2250 MW wind farm of the Capacity Expansion Scenario will exceed the borders of the project areas as well as the east border of Utsira Nord for this distance, illustrated in Fig. 3.4. From Fig. 5.2, this wind farm layout cause more wake effects compared to the uniform wind farm for the same turbine distance. These results imply that installing 2250 MW for the three projects areas using the upper range of the turbine distances are neither practically feasible, due to exceeding the borders of the designated areas, or beneficial for wake effects compared to a uniform area.

5.4 Effect of Turbine Distance

Since wake effects are more pronounced closer to the rotor and diminish with distance, increasing turbine distances significantly reduces wake loss in the lower range of higher capacity densities. This effect decreases as turbine distances increase, resulting in less improvement of wake losses for both approaches, as illustrated in section 4.2.2 and section 4.3.

The capacity assessment with a constant turbine distance provides a basis for comparing the results for a 7D turbine distance with alternative distances. Turbine distances from 2D-15D results in a farm power range from 720-849 MW for the Initial Scenario, with a corresponding wake loss from 19% to 4.4%. The wind farm results from using a 7D distance stated as 820 MW with a 7.7% wake loss (section 4.2.1) is thereby in the upper part of the power range while keeping wake loss relatively low. The power range increases to 1082-1304 MW for the Capacity Expansion Scenario and 1442-1729 MW for the Area Expansion Scenario, both with a wake loss ranging from 22% to 6%. Hence, the results from a 7D distance of 1256 MW and 1669 MW with associated wake loss of 9.5% and 9.8% is also in the upper power ranks and the lower wake loss ranks, especially for the Area Expansion Scenario. Comparing the results with estimations by The Norwegian Water Resources and Energy Directorate (2012b) for the same

area, the results are in acceptable agreement with the stated wake loss of 7% and 10% for an installed capacity of 504 MW and 1512 MW respectively.

The capacity density analysis for each approach show different effects on the internal and external wake effects with increasing turbine distances. Both approaches show an overall dominant ratio of internal wake loss that is more significant for lower turbine distances. Using a constant installed capacity (section 4.2.2) cause the external wake loss to increase with growing turbine distances, due to diminishing distance between the project areas as the wind farm area expand for longer distances between each turbine. In contrast, full utilization of the project areas in section 4.3 cause the external wake losses to decrease with growing turbine distance. This is expected as the number of turbines within each project area is reduced and generate less wake effects, while the distance between each area is constant.

5.5 Alternative Wind Farm Layout

Considering the prevailing wind direction when choosing the turbine distance will require less of the designated areas while reducing the wake loss and increasing the power production, compared to a constant 7D distance. The average wake loss for a single turbine within the wind farm is reduced from a range of 2.7-10% with a 7D distance (section 4.2.2) to 2-9% for the alternative layout of the Initial Scenario (section 4.2.3). This can be related to the clustering of the wind farms of each project area, avoiding centre turbines as each cluster only consist of two turbine rows. There is less improvement for the Capacity Expansion Scenario and the Area Expansion Scenario, with an average minimum of 3% for both the 7D and the alternative layout, while the average maximum is reduced from 13% to 12%. This is likely related to the reduced possibilities for wind farm clustering, due to more turbines and therefore less available space within the project areas. The total wake loss for the Initial Scenario is decreased by 1.3% from comparing Table 4.4 and Table 4.6, which increase the farm power by 11 MW. This increase outcome is equivalent to a yearly energy production of 96 GWh and is enough to power approximately 6400 households for a year. By considering the prevailing wind direction for the turbine distances in the Capacity Expansion Scenario and the Area Expansion Scenario, the total

wake loss is reduced by 0.5% and 0.8%, which increase the corresponding farm power by 7 MW and 15 MW and the yearly production by 61 GWh and 131 GWh. This can power about 4000 and 8700 homes respectively. Hence, the improvement in wind farm efficiency constitute a substantial contribution to the power production.

The effects from using the alternative layout for the wind farms are assessed further by separating the wake losses in external and internal wake. The ratio of internal wake loss and external wake loss is illustrated in Fig. 5.3 for Scenario 1 (Initial Scenario), 2 (Capacity Expansion Scenario) and 3 (Area Expansion Scenario) with the alternative layout versus a constant turbine distance of 7D. The figure reveal that the wake loss reduction for the Initial Scenario is mainly caused by reducing internal wake effects. Specifically, the internal wake loss is reduced by 1.2% while the external wake loss 0.1%. For the Capacity Expansion Scenario, the internal wake loss reduction is less significant (0.3%) while there is a slight greater reduction in external wake (0.2%). For the Area Expansion Scenario, there is a 0.5% reduction of internal wake loss and 0.3% of external wake loss. Thereby, the new layout for the fourth project area cause greater improvement for both internal and external wake compared to the Capacity Expansion Scenario.

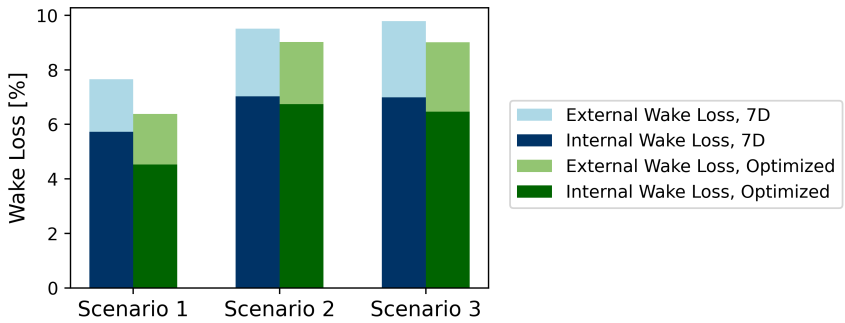

Figure 5.3: Internal and external wake loss for Scenario 1 (Initial Scenario), 2 (Capacity Expansion Scenario) and 3 (Area Expansion Scenario) with a 7D turbine distance versus an alternative layout of 5D within the turbine rows and 9D between them.

To further investigate the cause of these results, the wake loss reduction for each project area is examined. The internal wake loss is no longer constant

for each project area, as the alternative layout result in very different wind farm layout for each area. As shown in Fig. 5.3, the alternative layout of the Initial Scenario cause greater reduction of internal wake loss compared to the other scenarios. From Table 5.1, the improvement is most significant for Project area 1. This may be caused from placing the top left cluster further east, reducing the wake impact on the other clusters. For the Capacity Expansion Scenario and the Area Expansion Scenario with only two clusters in the three project areas of Utsira Nord, the overall wake loss reduction is less significant. The improvement for Project area 1 is greater than the two other project areas in Utsira Nord, which may be due to the first turbine row being placed with a four kilometer distance from the remaining rows. Project area 4 with four clusters, have a wake loss reduction similar to the project areas of the Initial Scenario. Thereby, the clustering of the fourth project area in the Area Expansion Scenario cause the original difference in wake loss from the Capacity Expansion Scenario to be negligible.

	Internal Wake Loss [%]	
	Alternative Layout	Reduction
Scenario 1		
Project area 1	4.45	1.25
Project area 2	4.6	1.1
Project area 3	4.6	1.1
Scenario 2		
Project area 1	6.6	0.4
Project area 2	6.9	0.1
Project area 3	6.8	0.2
Scenario 3		
Project area 1	6.6	0.4
Project area 2	6.9	0.1
Project area 3	6.8	0.2
Project area 4	5.7	1.2

Table 5.1: Internal wake loss for Scenario 1 (Initial Scenario), 2 (Capacity Expansion Scenario) and 3 (Area Expansion Scenario) with an alternative layout and the reduction from a constant 7D diameter.

These results suggest that there is a greater effect from division of clusters and turbine rows vertically, from comparing Project area 1 and Project area 4 with the remaining areas that is only separated lengthwise. This is expected as the dominant wind from north-northwest cause turbines to stand in the wake of turbines from upstream rows more frequently than neighbouring wind turbines in the same row. Hence, these results support the decision of increasing the distance between the turbine rows (9D) while using shorter distances within the rows (5D). This also imply that the division of project areas in this direction is favourable for wake losses, in addition to facilitating maritime traffic.

5.6 Power Potential in Utsira Nord

The installed capacities of Scenario 1 (Initial Scenario), 2 (Capacity Expansion Scenario) and 3 (Area Expansion Scenario) constitutes 4.8-10% of the governments ambition of 30 GW offshore wind production by 2040. The resulting power production is dependent on the turbine distance. As discussed in section 5.3, a 7D turbine distance is shown to be a good option for high production while keeping wake losses relatively low, as well as keeping the wind farm area within the designated areas. Considering wake effects, the yearly energy production for the wind farm of the Initial Scenario with a constant 7D turbine distance is estimated as 7.2 TWh. To put this in perspective, this is enough to provide nearly 480 thousand households with electricity for a year. A capacity expansion of 250 MW within each project area for the Capacity Expansion Scenario increase the annual production to 11.0 TWh, equivalent to the electricity need of more than 730 thousand households. By expanding the wind farm area by adding another project area of 750 MW for the Area Expansion Scenario, the wind farm can produce 12.6 TWh/year and supply more than 970 thousand households. As discussed in section 5.5, considering the prevailing wind direction for the distances between the turbines have significant effect on the wind farm wake, and cause substantial improvements for the power production. Using these wind farm layouts, the three scenarios can constitute a yearly production of 7.3 TWh, 11.1 TWh and 14.8 TWh. As shown in section 5.3, full utilization of the Utsira Nord area can offer further potential for capacity expansion.

Full utilization of the three project areas in Utsira Nord enables a yearly production of 14.2 TWh with a 7D turbine distance, 3.2 TWh more than for the Capacity Expansion Scenario using the same turbine distance and the same area. Decreasing the turbine distance to 4D is shown increase the production by 250%, which constitute 35.5 TWh/year. As stated in section 2.5, typical turbine distances in excising wind farms is stated as 6-10D by Stevens et al. (2016). Thereby, a 7D turbine distance is considered more realistic. Theoretically, a uniform wind farm that utilize all of Utsira Nord, without project areas, can produce 45.5 TWh/year with a 5D turbine distance and supply 3.0 million households. However, a 7D turbine distance is considered more realistic, which constitute 18% of the 30 GW government stated offshore wind ambition and a production of 25.2 TWh/year that could supply for 1.7 million households.

Chapter 6

Conclusions

This study investigate the offshore wind power potential in Utsira Nord by examining the effects of capacity expansion and turbine distance on the wind farm performance. Seasonal variations in turbulence intensity suggest that using a constant turbulence intensity for modelling can cause inaccuracies in seasonal production predictions. Modelling results reveal that increasing capacity within project areas cause more wake effects than adding additional areas. The installed capacities of Scenario 1 (Initial Scenario), 2 (Capacity Expansion Scenario) and 3 (Area Expansion Scenario) constitute 4.8-10% of the government's 30 GW offshore wind production ambition by 2040. Full utilization of Utsira Nord as a uniform wind farm offer further capacity expansion potential that would constitute 18% of the 30 GW ambition with a 7D turbine distance. Reducing turbine distance improve production for a given wind farm area, but increase wake losses.

In conclusion, the optimal turbine distance and installed capacity depend on the available area and the power requirement, as these parameters affect each other. However, important considerations that are obtained from the results include the significance of turbine spacing, wind farm clustering and wind farm orientation on the resulting wind farm wake. It is evident that clustering of smaller wind farms with sufficient spacing between them are more beneficial for wake loss compared to increasing capacity within existing areas. This imply promising effects for expanding the wind farm area to Vestavind F, as suggested by NVE. A 7D turbine distance is found to balance high production and low wake losses while staying within the designated areas. An alternative layout that consider the prevailing wind direction for the turbine distances reduce the wake losses further. Furthermore, wind farm orientation is shown to affect wind farm performance significantly, suggesting that the wind farms of the three defined project areas can benefit from considering the prevailing wind direction instead of following the area borders. Overall, the findings underscore the importance of capacity density and turbine placement for efficient ocean resource utilization.

The results of these studies are limited to wind farm layouts of turbine rows that are aligned in straight lines, rather than optimal positions. Additionally, the studies only consider the direct effects on wake loss and power production. There are numerous parameters that must be considered for a comprehensive evaluation of the optimal wind farm layout, including economical, environmental and other technological aspects. Future studies should investigate the effects of optimal turbine placement and wind farm orientation, as well as possibilities for control strategies to manipulate the wake trajectory. The technical results should be combined with economic aspects, such as considerations of investment and operational costs associated with increasing number of turbines.

Bibliography

Al Halabi, M. (2023). *Comparing wind farm production data to engineering wake model simulations*. Master's thesis Faculty of Technology, Natural sciences, and Maritime Sciences, Campus Porsgrunn.

Ann Christin Bøeng, Statistisk sentralbyrå (SSB) (2023). Hva er gjennomsnittlig strømforbruk i husholdningene? https://www.ssb.no/energi-og-industri/energi/artikler/hva-er-gjennomsnittlig-stromforbruk-i-husholdningene.

Bak, C., Zahle, F., Bitsche, R., Kim, T., Yde, A., Henriksen, L., Hansen, M., Blasques, J., Gaunaa, M., & Natarajan, A. (2013). The dtu 10-mw reference wind turbine. Danish Wind Power Research 2013 ; Conference date: 27-05-2013 Through 28-05-2013.

Barthelmie, R., Hansen, K. S., Frandsen, S., Rathmann, O., Schepers, J., Schlez, W., Phillips, J., Rados, K., Zervos, A., Politis, E., & Chaviaropoulos, P. (2009). Modelling and measuring flow and wind turbine wakes in large wind farms offshore. *Wind Energy*, *12*, 431 – 444. doi:10.1002/we.348.

Barthelmie, R. J., & Jensen, L. E. (). Evaluation of wind farm efficiency and wind turbine wakes at the nysted offshore wind farm. *Wind Energy*, *13*, 573–586. URL: https://onlinelibrary.wiley.com/doi/abs/10.1002/we.408. doi:https://doi.org/10.1002/we.408. arXiv:https://onlinelibrary.wiley.com/doi/pdf/10.1002/we.408.

Bastankhah, M., & Porté-Agel, F. (2014). A new analytical model for wind-turbine wakes. *Renewable Energy*, *70*, 9938–. doi:10.1016/j.renene.2014.01.002.

Bastankhah, M., & Porté-Agel, F. (2016). Experimental and theoretical study of wind turbine wakes in yawed conditions. *Journal of Fluid Mechanics*, *806*, 506–541. doi:10.1017/jfm.2016.595.

Betz, A. (1926). *Wind-Energie und ihre Ausnutzung durch Windmühlen*. Göttingen: Vandenhoeck & Ruprecht.

Frandsen, S. (2007). *Turbulence and turbulence-generated structural loading in wind turbine clusters*. Ph.D. thesis. Risø-R-1188(EN).

Gaertner, E., Rinker, J., Sethuraman, L., Zahle, F., Anderson, B., Barter, G., Abbas, N., Meng, F., Bortolotti, P., Skrzypinski, W., Scott, G., Feil, R., Bredmose, H., Dykes, K., Shields, M., Allen, C., & Viselli, A. (2020). *Definition of the IEA 15-Megawatt Offshore Reference Wind Turbine*. National Renewable Energy Laboratory (NREL).

Gayle Nygaard, N., Steen, S., Poulsen, L., & Grønnegaard Pedersen, J. (2020). Modelling cluster wakes and wind farm blockage. *Journal of Physics: Conference Series*, *1618*, 062072. doi:10.1088/1742-6596/1618/6/062072.

Giebel, G., & Hasager, C. (2016). An overview of offshore wind farm design. (pp. 337–346). doi:10.1007/978-3-319-39095-6_19.

Global Wind Energy Council (2024). Global wind report 2024. URL: https://gwec.net/global-wind-report-2024 accessed: 2024-05-21.

Haakenstad, H., Øyvind Breivik, Furevik, B. R., Reistad, M., Bohlinger, P., & Aarnes, O. J. (2021). Nora3: A nonhydrostatic high-resolution hindcast of the north sea, the norwegian sea, and the barents sea. *Journal of Applied Meteorology and Climatology*, *60*, 1443 – 1464. URL: https://journals.ametsoc.org/view/journals/apme/60/10/JAMC-D-21-0029.1.xml. doi:10.1175/JAMC-D-21-0029.1.

Hasager, C. B., Vincent, P., Badger, J., Badger, M., Di Bella, A., Peña, A., Husson, R., & Volker, P. J. H. (2015). Using satellite sar to characterize the wind flow around offshore wind farms. *Energies*, *8*, 5413–5439. URL: https://www.mdpi.com/1996-1073/8/6/5413. doi:10.3390/en8065413.

International Energy Agency (2021). Renewables information: Overview. URL: https://www.iea.org/reports/renewables-information-overview licence: CC BY 4.0.

International Energy Agency (2024). Renewables 2023. URL: https://www.iea.org/reports/renewables-2023 licence: CC BY 4.0.

Jacobson, M., & Archer, C. (2012). Saturation wind power potential and its implications for wind energy. *Proceedings of the National Academy of Sciences of the United States of America*, *109*, 15679–84. doi:10.1073/pnas.1208993109.

Jensen, N. (1983). *A note on wind generator interaction*. Number 2411 in Risø-M. Risø National Laboratory.

JM, J., Butterfield, S., Musial, W., & Scott, G. (2009). Definition of a 5mw reference wind turbine for offshore system development. *National Renewable Energy Laboratory (NREL)*, . doi:10.2172/947422.

Kaimal, J. C., & Finnigan, J. J. (1994). *Atmospheric Boundary Layer Flows: Their Structure and Measurement*. New York: Oxford Academic. URL: https://doi.org/10.1093/oso/9780195062397.001.0001 online edition accessed 17 May 2024.

Katic, I., Højstrup, J., & Jensen, N. (1987). A simple model for cluster efficiency. In W. Palz, & E. Sesto (Eds.), *EWEC'86. Proceedings. Vol. 1* (pp. 407–410). A. Raguzzi. European Wind Energy Association Conference and Exhibition, EWEC '86 ; Conference date: 06-10-1986 Through 08-10-1986.

Lanzilao, L., & Meyers, J. (2022). A new wake-merging method for wind-farm power prediction in the presence of heterogeneous background velocity fields. *Wind Energy*, *25*, 237–259. URL: https://onlinelibrary.wiley.com/doi/abs/10.1002/we.2669. doi:https://doi.org/10.1002/we.2669. arXiv:https://onlinelibrary.wiley.com/doi/pdf/10.1002/we.2669.

Larsen, G., Madsen Aagaard, H., Bingöl, F., Mann, J., Ott, S., Sørensen, J., Okulov, V., Troldborg, N., Nielsen, N., Thomsen, K., Larsen, T., & Mikkelsen, R. (2007). *Dynamic wake meandering modeling*. Number 1607(EN) in Denmark. Forskningscenter Risoe. Risoe-R. Risø National Laboratory.

Larsén, X. (2022). *Calculating Turbulence Intensity from mesoscale modeled Turbulence Kinetic Energy*. Number E-0233 in DTU Wind Energy E. DTU Wind and Energy Systems.

Lissaman, P. (1979). Energy effectiveness of arbitrary arrays of wind turbines. In *17th Aerospace Sciences Meeting*. URL: https://arc.aiaa.org/doi/abs/10.2514/6.1979-114. doi:10.2514/6.1979-114. arXiv:https://arc.aiaa.org/doi/pdf/10.2514/6.1979-114.

Nielsen, F. G. (2024). *Environmental Conditions and Dynamics of Fixed and Floating Turbines*. Cambridge University Press.

Norwegian Institute for Nature Research (2012). *Tilstand og utvikling for biologisk mangfold i Norge*. Technical Report Norsk institutt for naturforskning (NINA). URL: https://www.nina.no/archive/nina/pppbasepdf/rapport/2012/825.pdf.

Nouri, R., Nash, R., & Vasel-Be-Hagh, A. (2022). Wind turbine wake redirection via external vanes. (pp. 61–71). doi:10.1007/978-3-031-20506-4_3.

Nybø, A., Nielsen, F. G., Reuder, J., Churchfield, M. J., & Godvik, M. (). Evaluation of different wind fields for the investigation of the dynamic response of offshore wind turbines. *Wind Energy*, *23*, 1810–1830. URL: https://onlinelibrary.wiley.com/doi/abs/10.1002/we.2518. doi:https://doi.org/10.1002/we.2518. arXiv:https://onlinelibrary.wiley.com/doi/pdf/10.1002/we.2518.

Nygaard, N. G., Poulsen, L., Svensson, E., & Pedersen, J. G. (2022). Large-scale benchmarking of wake models for offshore wind farms. *Journal of Physics: Conference Series*, *2265*, 022008. URL: https://dx.doi.org/10.1088/1742-6596/2265/2/022008. doi:10.1088/1742-6596/2265/2/022008.

Parada, L., Herrera, C., Flores, P., & Parada, V. (2017). Wind farm layout optimization using a gaussian-based wake model. *Renewable Energy*, *107*, 531–541. URL: https://www.sciencedirect.com/science/article/pii/S0960148117300952. doi:https://doi.org/10.1016/j.renene.2017.02.017.

Pedersen, J. G., Svensson, E., Poulsen, L., & Nygaard, N. G. (2022). Turbulence optimized park model with gaussian wake profile. *Journal of Physics: Conference Series*, *2265*, 022063. URL: https:

//dx.doi.org/10.1088/1742-6596/2265/2/022063. doi:10.1088/1742-6596/2265/2/022063.

Platis, A., Siedersleben, S., Bange, J., Lampert, A., Bärfuss, K., Hankers, R., Canadillas, B., Foreman, R., Schulz-Stellenfleth, J., Djath, B., Neumann, T., & Emeis, S. (2018). First in situ evidence of wakes in the far field behind offshore wind farms. *Scientific Reports*, *8*, 2163. doi:10.1038/s41598-018-20389-y.

Popko, W., Thomas, P., Sevim, A., Rosemeier, M., Bätge, M., Braun, R., Meng, F., Horte, D., Balzani, C., Bleich, O., Daniele, E., Stoevesandt, B., Kuhn, M., Polman, J., Leimeister, M., Schümann, B., & Reuter, A. (2018). Iwes wind turbine iwt-7.5-164 rev 4. doi:10.24406/IWES-N-518562.

Porté-Agel, F., Bastankhah, M., & Shamsoddin, S. (2020). Wind-turbine and wind-farm flows: A review. *Boundary-Layer Meteorology*, *174*, 1–59. URL: https://doi.org/10.1007/s10546-019-00473-0. doi:10.1007/s10546-019-00473-0.

Porté-Agel, F., Wu, Y.-T., & Chen, C.-H. (2013). A numerical study of the effects of wind direction on turbine wakes and power losses in a large wind farm. *Energies*, *6*, 5297–5313. URL: https://www.mdpi.com/1996-1073/6/10/5297. doi:10.3390/en6105297.

Schmidt, J., & Vollmer, L. (2020). Industrial wake models. In B. Stoevesandt, G. Schepers, P. Fuglsang, & S. Yuping (Eds.), *Handbook of Wind Energy Aerodynamics* (pp. 1–28). Cham: Springer International Publishing. URL: https://doi.org/10.1007/978-3-030-05455-7_49-1. doi:10.1007/978-3-030-05455-7_49-1.

Schmidt, J., Vollmer, L., Dörenkämper, M., & Stoevesandt, B. (2023). Foxes: Farm optimization and extended yield evaluation software. *Journal of Open Source Software*, *8*, 5464. URL: https://doi.org/10.21105/joss.05464. doi:10.21105/joss.05464.

Schubel, P., & Crossley, R. (2014). Wind turbine blade design. (pp. 1–34). doi:10.1201/b16587-3.

Simley, E., Angelou, N., Mikkelsen, T., Sjöholm, M., Mann, J., & Pao, L. (2016). Characterization of wind velocities in the upstream induction zone

of a wind turbine using scanning continuous-wave lidars. *Journal of Renewable and Sustainable Energy*, *8*, 013301. doi:10.1063/1.4940025.

Skrzypiński, W., Bech, J., Hasager, C., Tilg, A. M., & Bak, F. (2020). Optimization of the erosion-safe operation of the iea wind 15 mw reference wind turbine. *Journal of Physics: Conference Series*, *1618*, 052034. doi:10.1088/1742-6596/1618/5/052034.

Solbrekke, I. M., Sorteberg, A., & Haakenstad, H. (2021). The 3 km norwegian reanalysis (nora3) – a validation of offshore wind resources in the north sea and the norwegian sea. *Wind Energy Science*, *6*, 1501–1519. URL: https://wes.copernicus.org/articles/6/1501/2021/. doi:10.5194/wes-6-1501-2021.

Stevens, R., Hobbs, B., Ramos, A., & Meneveau, C. (2016). Combining economic and fluid dynamic models to determine the optimal spacing in very large wind farms. *Wind Energy*, *20*. doi:10.1002/we.2016.

Stieren, A., & Stevens, R. (2021). Evaluating wind farm wakes in large eddy simulations and engineering models. *Journal of Physics: Conference Series*, *1934*, 012018. doi:10.1088/1742-6596/1934/1/012018.

The Norwegian Government (). Utsira nord. URL: https://www.regjeringen.no/no/tema/energi/landingssider/havvind/utsira-nord/id2967232/.

The Norwegian Water Resources and Energy Directorate (2012a). *Evaluering av energiressurser i norsk fastlandsområde. NVEs arbeid med regionalisert vind- og solenergiutredning (RESS 2012)*. Technical Report Norges vassdrags- og energidirektorat (NVE). URL: https://publikasjoner.nve.no/rapport/2012/rapport2012_47.pdf.

The Norwegian Water Resources and Energy Directorate (2012b). *HAVVIND Strategisk konsekvensutredning*. Technical Report Norges vassdrags- og energidirektorat. URL: https://publikasjoner.nve.no/rapport/2012/rapport2012_47.pdf.

The Norwegian Water Resources and Energy Directorate (2018). *Bilag til SSA-O – Oppdragsavtalen – versjon april 2018, Fagutredning for*

virkninger av havvind for kraftproduksjon og vindregime. Technical Report.

The Norwegian Water Resources and Energy Directorate (2023). Vestavind f (inkludert utsira nord). URL: https://veiledere.nve.no/havvind/identifisering-av-utredningsomrader-for-havvind/nye-omrader-for-havvind/vestavind-f-inkl-utsira-nord/.

The Royal Ministry of Petroleum and Energy (2023). Utlysning av konkurranse om prosjektområder i utsira nord til fornybar energiproduksjon til havs. URL: https://www.regjeringen.no/contentassets/94b9f178d05849a1a5852ce129693f27/utlysningsdokument-utsira-nord.pdf.

Vattenfall (). Horns Rev 3 — Powerplants — Vattenfall. https://powerplants.vattenfall.com/horns-rev-3/. Accessed: April 26, 2024.

Volker, P. J. H., Hahmann, A. N., Badger, J., & Jørgensen, H. E. (2017). Prospects for generating electricity by large onshore and offshore wind farms. *Environmental Research Letters*, *12*, 034022. URL: https://dx.doi.org/10.1088/1748-9326/aa5d86. doi:10.1088/1748-9326/aa5d86.